Canadian Contractor Report of

Hydrography and Ocean Sciences No. xxx

1986

TIDAL CIRCULATION OF THE SCOTIAN SHELF AND GRAND BANKS

by

Sylvain de Margerie

and

Karen D. Lank

ASA Consulting Ltd.

P. O. Box 2025

Dartmouth East, Nova Scotia

B2W 3X8

Prepared under contract no. 08SC.FP901-5-X515

for the Department of Fisheries and Oceans

Canadian Contractor Report of

Hydrography and Ocean Sciences No. xxx

1986

TIDAL CIRCULATION OF THE SCOTIAN SHELF AND GRAND BANKS

by

Sylvain de Margerie

and

Karen D. Lank

ASA Consulting Ltd.

P. O. Box 2025

Dartmouth East, Nova Scotia

B2W 3X8

Prepared under contract no. 08SC.FP901-5-X515

for the Department of Fisheries and Oceans

TABLE OF CONTENTS

LIST OF FIGURES

LIST OF TABLES

ABSTRACT

Numerical modelling of the barotropic tidal circulation was undertaken for the Scotian Shelf and the Grand Banks primarily for the purpose of assessing the potential for internal wave generation on the edge of the continental shelf. The results, however, are generally useful from an oceanographic point of view, because barotropic tidal currents account for a substantial fraction of the current variance. It is shown that simulation of the M2, K1 and O1 tides, with no nonlinear interaction, is sufficient to describe the tidal circulation for the region of concern. Error analysis shows that model accuracy is comparable to observational uncertainty. Final results are presented in terms of cotidal charts and tidal ellipses for the M2, K1 and O1 constituents. Also shown are contours of a forcing factor for internal tides, which may be used as an indicator of high internal wave activity.

RESUME

La circulation barotropique due à la marée est simulée au moyen d'un modèle mathématique, avec le but principal de déterminer le potentiel pour la génération d'ondes internes sur le rebord du Plateau Scotian et des Grands Bancs. Ces résultats sont toute fois d'intérêt général en océanographie, étant donné que les marées sont responsable pour une grande partie des courrants sur le plateau continental. On démontre que des simulations indépendantes (sans intéraction nonlinéaire) pour les composantes de marée M2, K1 et O1 suffisent à décrir la circulation dans la région d'étude. Une comparaison des résultats de simulation avec des observations nous permet d'établir que la précision du modèle est comparable à la marge d'erreur observationelle. Les résultats sont présentés sous forme d'isoplete d'amplitude et de phase, ainsi que par des élipses de marée pour les composantes M2, K1 et O1. On présente également des contours d'un facteur de forçage pour la marée interne pouvant servir d'index pour le potentiel de génération d'ondes internes.

ACKNOWLEDGEMENTS

The numerical model forming the basic tool for this study is largely based on the work of David Greenberg, who provided valuable assistance in its development and application. Simulations for the Grand Banks were first undertaken by Brian Petrie, whose work has greatly simplified our task. We are also grateful to Shell Canada Resources Ltd. and Mobil Oil Canada Ltd. for allowing us to use their current meter data for the verification of our results. Many thanks are due to Jim Elliott and Hal Sandstrom who supervised the project and were responsible for securing funding.

1. INTRODUCTION

Recent observations on the Scotian Shelf and Grand Banks (Sandstrom and Elliott, 1984) have shown the presence of large amplitude internal waves of tidal origin. It has been shown by several authors (Rattray, 1960; Wunsch, 1975) that the principal generation mechanism for internal waves of tidal period is the disturbance of the density field caused by currents associated with the surface tide as they flow over changing topography. The primary goal of the present numerical investigation is to quantify the barotropic (surface) tidal circulation on the Scotian Shelf in order to better define the causal mechanisms for internal waves. Since tides account for up to half of the total current variance (Petrie, 1982; Smith, Petrie and Mann, 1978), the results of such a numerical investigation are also of general interest and are an improvement over descriptions of the tidal circulation derived from observations alone (Moody et al., 1984). The results presented herein summarize several years of work involving model development and applications. The interested reader is directed to earlier reports for more detailed discussions.

2. MODELLING METHODOLOGY

The numerical model used to simulate tidal circulation on the Scotian Shelf and the Grand Banks has been described elsewhere (de Margerie, 1985). It solves the fully nonlinear equations of motion in spherical coordinates, using a semi-implicit method similar to that of Greenberg (1983). The model

resolution is 4' by 4' (approximately 7 by 5 kilometers). Due to the large computational requirements, the Scotian Shelf and the Grand Banks were simulated independently, with a common boundary along the Laurentian Channel (Figures 1 and 2). Model boundaries were set well beyond the 200-m isobath in the offshore direction so that constraints imposed on the boundary would have minimal effects on circulation at the shelf edge, where internal waves are generated. Elevation conditions for open boundaries are derived primarily from observations. In the case where stations are not located along the model perimeter, a certain amount of iterative adjustment is done until computed elevations agree with observations at nearby sites inside the model domain.

Sensitivity analysis to the formulation and degree of dissipation (bottom friction and horizontal viscosity) has shown that model results are relatively independent of these parameters. This result is supported from a theoretical point of view if we consider that the spin down time for a continental shelf, estimated as $\frac{KV}{2h}$ (where $K \simeq 0.003$ is the bottom friction coefficient, $V \simeq 0.2$ m/s is a velocity scale and $h \simeq 150$ m is the water depth), is on the order of 6 days, which is long compared to the time scale of tidal motion. A quadratic friction with a coefficient of 0.0023 is representative of dissipation normally used in continental shelf modelling and is used throughout our simulations. A small component of linear friction as well as depth dependent eddy viscosity is also included (see de Margerie, 1985) to improve numerical stability.

Although the model solves the fully nonlinear equations of motion, it can be shown that nonlinearity does not play a crucial role in tidal propagation

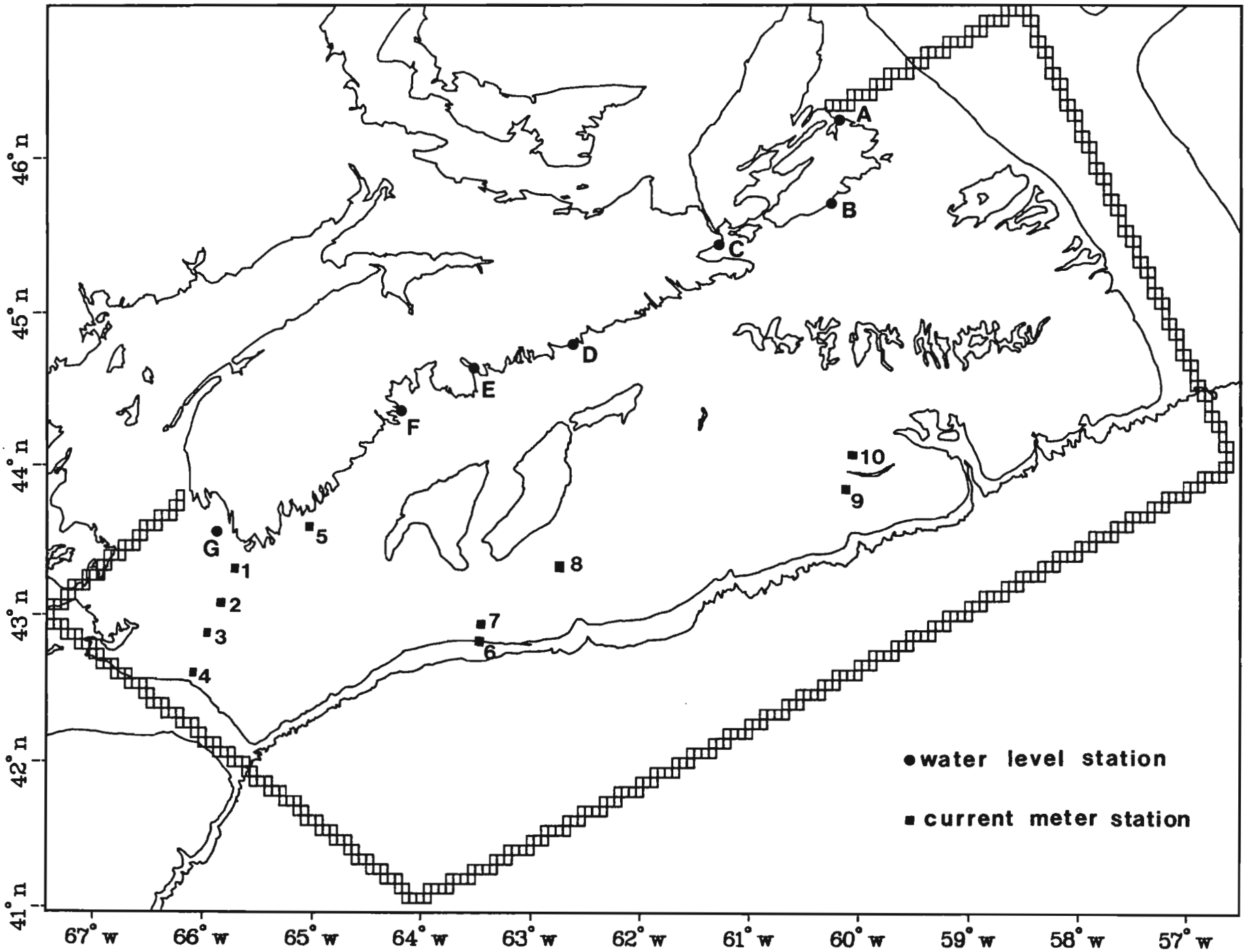

FIGURE 1 Model Domain for the Scotian Shelf, also shown are the locations of stations used for comparison with observations.

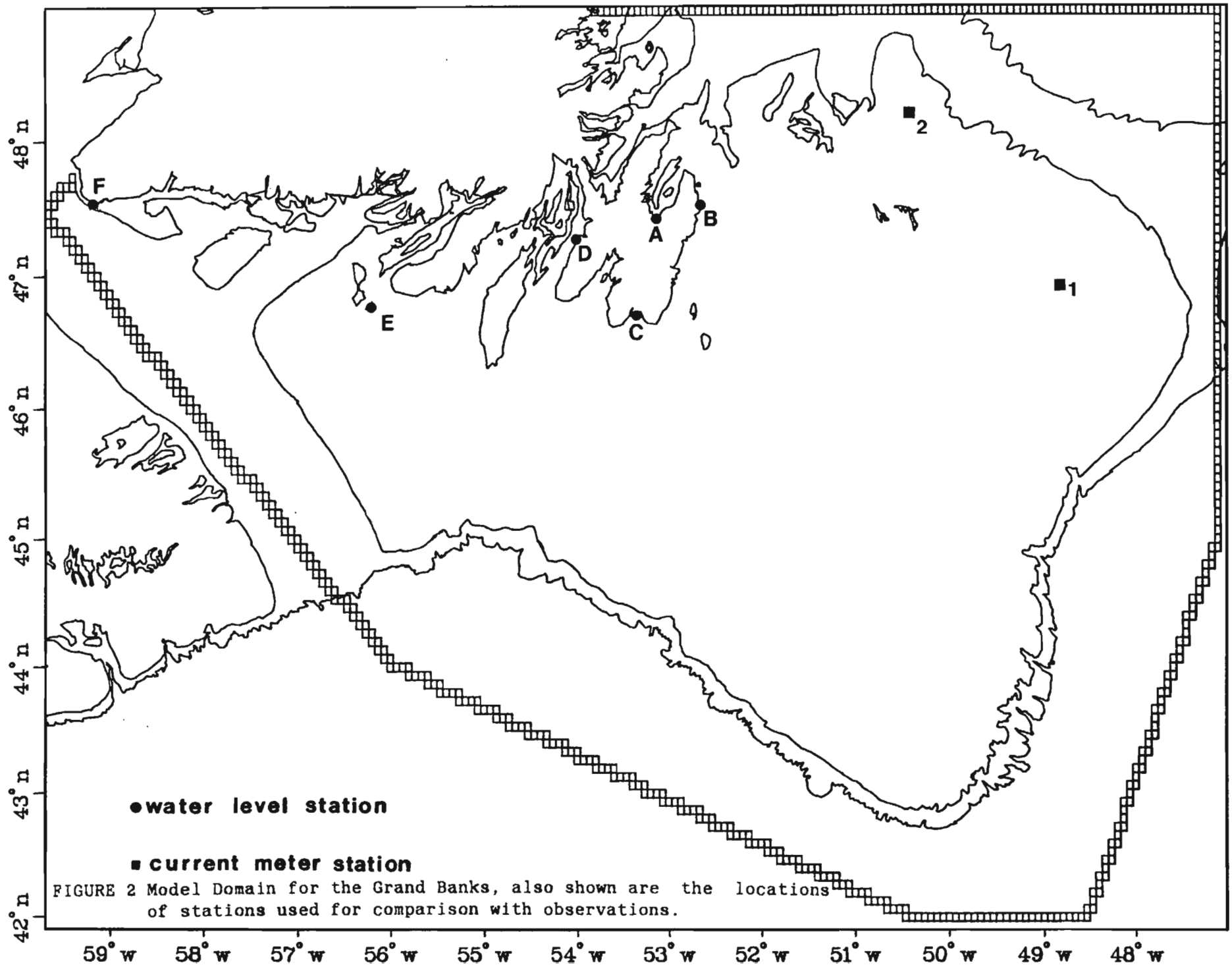

FIGURE 2 Model Domain for the Grand Banks, also shown are the locations of stations used for comparison with observations.

over the study regions. Nonlinearity is introduced in the continuity equation when the water level fluctuation is a considerable fraction of the water depth, and in the momentum equation through advective and quadratic friction terms. The tidal range in the study area is much less than the water depth, and as discussed above friction does not play a major role. Using a velocity scale of 0.2 m/s and a length scale equal to the shelf width (150 km), we find that advective terms are two orders of magnitude smaller than other components of motion for the M2 tide. We can therefore conclude that nonlinear effects are negligible and each tidal constituent can be considered independently (without nonlinear interactions).

3. SELECTION OF TIDAL CONSTITUENTS

In view of the very large computational requirement of the model it is important to minimize the number of runs. Since each tidal constituent will be simulated individually this means we should determine the minimum number of constituents necessary to realistically reproduce the tidal regime on the shelf. Considering Halifax as a typical coastal station we find that the five largest constituents (excluding the annual cycle) are M2, N2, S2, K1 and O1, in all accounting for 98% of the tidal variance. We will therefore restrict our attention to these constituents.

It is common practice in tidal analysis and prediction to infer the behaviour of secondary constituents from main ones, suggesting that simulations for even fewer constituents may be adequate. In order to investigate the relationship between principal and secondary tidal

constituents in the diurnal and semi-diurnal bands, we have computed amplitude ratios and phase differences, known as inference parameters, for the M2:N2:S2 and K1:O1 groups. Table 1 shows these values plus mean and standard deviations for main shore stations ordered from north to south along the coast. We find that the N2 tide, which is closest in frequency to the M2, is in fact consistently related to it, with variations in amplitude ratio and phase difference commensurate with observational uncertainties (to be discussed in the following section). The variability in amplitude ratio for the other constituents is larger, but the errors introduced by the use of inference (less than 0.05 m) remain of the same order as the amplitude of lesser constituents which we have neglected altogether. Examining the spatial dependence of amplitude ratios we find that S2:M2 shows a definite decreasing trend from north to south, while O1:K1 has a localized minimum on the Scotian Shelf. Taking advantage of this we can reduce the error further by dividing the stations into two groups corresponding to the Newfoundland and Nova Scotia coasts and using separate inference parameters for each region. Using this technique, computations of tidal elevation using the M2 and K1, with the N2, S2 and O1 obtained by inference, will account for the major portion (97%) of the tidal elevation signal.

In modelling the tidal circulation we must consider that the distribution of variance among tidal constituents for currents may be different than that for elevations. Examination of available current data (Smith, 1983 and Petrie, 1982, for example) shows that the amplitude ratios and phase differences for N2:M2, S2:M2 and O1:K1 currents are similar to those for

TABLE 1

Inference Parameters for the Main
Diurnal and Semi-Diurnal Constituents

Amplitude Ratios (Phase differences)

	N2/M2(N2 - M2)	S2/M2(S2 - M2)	O1/K1(O1 - K1)
Newfoundland			
Holyrood	0.206(-15.3)	0.423(41.0)	0.873(-42.5)
St. John's	0.199(-17.5)	0.413(45.6)	0.901(-33.1)
Trepassey	0.186(-18.5)	0.292(55.3)	0.988(-23.7)
Argentia	0.220(-17.1)	0.287(34.2)	1.169(-17.8)
Port aux Basques	0.221(-18.6)	0.299(32.5)	1.160(-17.7)
Nova Scotia			
North Sydney	0.296(-20.7)	0.207(40.2)	1.065(-33.0)
Sandy Point	0.200(-24.3)	0.227(39.9)	0.597(-64.8)
Murphy Cove	0.223(-19.1)	0.208(30.8)	0.412(-31.5)
Halifax	0.221(-21.3)	0.220(28.1)	0.367(-24.1)
Lunenburg	0.234(-19.4)	0.213(23.3)	0.545(-10.3)
Seal Island	0.209(-26.0)	0.175(30.0)	0.963(-12.0)
Mean Inference Parameters for the whole Study Area	0.211(-19.8)	0.278(36.4)	0.822(-46.2)
Standard Deviation	0.013(3.0)	0.077(8.6)	0.278(36.0)
Typical Inference Error in meters			
in Newfoundland	0.005	0.028	0.023
in Nova Scotia	0.008	0.048	0.029
Mean Inference Parameters for Newfoundland	0.206(-17.4)	0.343(41.7)	1.018(27.0)
Standard Deviation	0.013(1.2)	0.062(8.3)	0.125(9.6)
Typical Inference Error in meters	0.005	0.022	0.010
Mean Inference Parameters for Nova Scotia	0.215(-21.8)	0.223(32.0)	0.658(-29.3)
Standard Deviation	0.011(2.5)	0.036(6.4)	0.264(18.1)
Typical Inference Error in meters	0.007	0.022	0.026

elevations. This can be expected as constituents of a similar frequency should propagate in similar fashions, with consistent relationships between elevation and currents.

The relative importance of diurnal and semi-diurnal amplitude is greater when considering currents, with K1:M2 typically 0.6 for current, compared to 0.15 for elevation. This behaviour is due to fundamental differences in the nature of the tidal disturbances, with the diurnal constituents having a major amphidromic system on the Scotian Shelf. Because the amplitude of diurnal currents is large, the error caused by inference of the O1 from the K1 constituent also becomes substantial. In considering tidal circulation it is therefore more appropriate to consider the K1 and O1 constituents individually. For the semi-diurnal constituents we suggest using the inference parameters derived for N2 and S2 elevations since these estimates are more accurate than those which can be obtained from current data. Using current meter data from the Grand Banks (Petrie, 1982) we find that approximately 94% of the tidal current variance can be accounted for by the M2, K1 and O1 with inference of the N2 and S2. Simulations will therefore be undertaken for the M2, K1 and O1 constituents.

4. ERROR ANALYSIS AND VERIFICATION

The accuracy of model predictions will be estimated by comparing the results of simulations to observed tidal elevations. Further verification will be undertaken by comparing predicted and observed currents.

First, let us consider the observational accuracy of tidal elevation to provide a scale for the success of numerical simulation. We will use Halifax as a basis for this analysis because it is a long standing tidal station with high quality observational records. Table 2 lists amplitudes and phases obtained from eleven different years of observation at Halifax. Each record consisted of 369 days of observations and was analyzed in a similar fashion. Also listed are mean and standard deviations computed from the 11 estimates of the M2, N2, S2, K1 and O1 constants. The observational uncertainty in amplitude (estimated as the standard deviation of the 11 yearly values) is in the order of 0.01 m for the M2 and 0.003 m for the other constituents. Similarly, the uncertainty in phase varies from about 1^{o} to 3^{o}.

Halifax is exceptional in that long records of tidal elevation are available. Other coastal stations used for verification of the numerical simulation typically had record lengths on the order of 80 days. It is readily shown that the observational error is inversely proportional to the square root of the record length (Godin, 1972). Therefore, assuming that all tidal stations have the same accuracy as Halifax (which may be optimistic) and are measuring similar signals, we can expect the observational uncertainties for the stations used in tidal model verification to be twice the standard deviations shown in Table 2.

Table 3 shows a comparison of observational uncertainty and simulation agreement for the M2, K1 and O1 tides. It can be seen that most of the discrepancy between the numerical simulations and observations is attributable

TABLE 2

Statistics of Tidal Observations for Halifax

Tidal Constant for Halifax from Different Years
(amplitudes in meters and phases in degrees)

Year	O1		K1		N2		S2		M2	
	AMP	PH	AMP	PH	AMP	PH	AMP	PH	AMP	PH
1964	0.046	38.2	0.108	62.5	0.139	213.0	0.140	262.4	0.634	234.6
1965	0.050	40.7	0.107	63.3	0.144	213.6	0.139	262.3	0.636	234.9
1966	0.050	37.0	0.104	60.5	0.145	214.1	0.141	261.7	0.632	234.2
1967	0.047	37.0	0.103	60.6	0.142	214.8	0.143	261.2	0.630	233.2
1968	0.046	36.8	0.104	62.0	0.143	216.2	0.139	263.3	0.637	234.3
1969	0.049	41.9	0.100	62.2	0.137	218.1	0.140	264.2	0.633	235.7
1970	0		0.099	59.8	0.136	215.6	0.132	262.9	0.608	233.8
1971	0.046	31.4	0.104	63.8	0.149	217.1	0.139	263.0	0.624	234.6
1972	0.046	31.7	0.103	62.7	0.143	217.0	0.138	264.1	0.623	235.8
1975	0.048	36.4	0.108	61.1	0.136	215.2	0.138	262.5	0.630	234.4
1976	0.040	38.7	0.108	62.8	0.140	213.1	0.139	262.5	0.633	234.4
Mean	0.046	37.1	0.105	62.0	.141	215.1	0.139	262.7	0.629	234.5
Standard Deviation*	0.003	3.1	0.003	1.2	.004	1.7	0.002	0.8	0.008	0.7

* The overall error for stations used in model verification is estimated at twice this standard deviation.

TABLE 3

Comparison of Modelled and Observed Tidal Elevation Parameters

	modelled (observed)					
	M2		K1		O1	
STATION	AMP.*	PHA.*	AMP.	PHA.	AMP.	PHA.
Newfoundland:						
A. Holyrood	0.356	312	0.085	171	0.067	131
	(0.352)	(?)	(0.079)	(?)	(0.069)	(?)
B. St. John's	0.368	315	0.081	172	0.069	132
	(0.356)	(317)	(0.081)	(162)	(0.073)	(128)
C. Trepassey	0.534	327	0.068	185	0.086	144
	(0.558)	(?)	(0.081)	(?)	(0.080)	(?)
D. Argentia	0.673	340	0.055	183	0.078	160
	(0.696)	(339)	(0.077)	(183)	(0.090)	(165)
E. Saint Pierre	0.597	350	0.046	190	0.060	178
	(0.603)	(348)	(0.060)	(195)	(0.073)	(177)
F. Port aux Basques	0.400	10	0.085	248	0.088	241
	(0.438)	(14)	(0.081)	(244)	(0.094)	(230)
Standard Error	0.017	2	0.010	5	0.006	6
Nova Scotia:						
A. North Sydney	0.381	355	0.076	323	0.103	289
	(0.368)	(353)	(0.077)	(325)	(0.082)	(287)
B. Louisbourg	0.493	344	0.067	18	0.057	326
	(0.502)	(344)	(0.060)	(24)	(0.060)	(321)
C. Sandy Point	0.560	344	0.070	43	0.051	344
	(0.596)	(344)	(0.072)	(53)	(0.043)	(346)
D. Murphy Cove	0.643	348	0.090	111	0.042	83
	(0.611)	(344)	(0.097)	(106)	(0.040)	(69)
E. Halifax	0.667	349	0.100	122	0.053	97
	(0.633)	(351)	(0.105)	(122)	(0.040)	(94)
F. Lunenberg	0.687	353	0.110	135	0.061	115
	(0.633)	(350)	(0.112)	(128)	(0.061)	(113)
G. Seal Island	1.287	53	0.125	178	0.106	159
	(1.203)	(52)	(0.137)	(179)	(0.103)	(163)
Standard Error	0.037	2	0.005	5	0.008	5

* Amplitudes are in meters and phases are Greenwich phase lag in degrees.

to observational error. The remaining difference can be attributed to the limited resolution of the model (i.e., model results represent average values for a grid cell of approximately 7 by 5 km and may be different from values at a given point within the cell).

Comparison of predicted and observed currents was also undertaken for several sites. Meaningful comparisons can only be made if measurements are available at enough depths to obtain accurate assessment of the depth-averaged tidal currents. A detailed description of the methodology used to obtain estimates of the barotropic tidal currents from observations is given in de Margerie (1985). The model does not resolve all bathymetric features and the water depth at current meter stations may differ from the mean depth of a model cell. To account for this, the model results are adjusted in order to preserve the integrated flux for a depth equal to the mooring site, so that we are effectively comparing tidal flux instead of tidal velocity.

Table 4 summarizes the comparison of observed and modelled tidal current parameters. The uncertainty in these current estimates was assessed by considering the repeatability of observations, signal contamination by wave action and the possible error introduced in the depth averaging process. As can be seen, model predictions are generally within observational accuracy. Because tidal currents and elevations are directly related we can expect the relative accuracy of current predictions to be as good as elevation prediction.

TABLE 4

Comparison of Modelled and Observed Tidal Current Parameters.

modelled
(observed)

STATION	M2 A*	M2 B*	M2 <*	M2 P*	M2 ±*	K1 A	K1 B	K1 <	K1 P	K1 ±	O1 A	O1 B	O1 <	O1 P	O1 ±
Grand Banks															
1	0.08	0.05	88	59c		0.03	0.02	72	4c		0.02	0.02	45	267c	
	(0.07)	(0.04)	(89)	(244c)	(0.01)	(0.03)	(0.03)	(96)	(358c)	(0.01)	(0.02)	(0.02)	(104)	(291c)	(0.01)
2	0.06	0.02	70	51c		0.02	0.01	103	287c		0.01	0.01	45	272c	
	(0.09)	(0.05)	(71)	(65c)	(0.02)	(0.03)	(0.02)	(121)	(322c)	(0.01)	(0.01)	(0.00)	(24)	(38c)	(0.01)
Scotian Shelf															
1	0.79	0.00	105	160c		0.11	0.04	87	355c		0.08	0.01	95	286c	
	(0.66)	(0.04)	(104)	(151c)	(0.03)	(0.06)	(0.01)	(80)	(326c)	(0.02)	(0.06)	(0.01)	(85)	(279c)	(0.02)
2	0.60	0.00	108	176a		0.07	0.03	80	2c		0.05	0.00	90	302a	
	(0.60)	(0.02)	(108)	(169c)	(0.03)	(0.05)	(0.01)	(82)	(342c)	(0.02)	(0.06)	(0.01)	(90)	(293c)	(0.02)
3	0.54	0.04	116	179c		0.06	0.03	66	356c		0.04	0.01	94	301c	
	(0.49)	(0.07)	(119)	(170c)	(0.03)	(0.04)	(0.00)	(68)	(350c)	(0.02)	(0.04)	(0.01)	(175)	(304c)	(0.02)
4	0.47	0.08	124	182c		0.11	0.06	68	16c		0.04	0.01	86	312c	
	(0.46)	(0.20)	(125)	(176c)	(0.02)	(0.05)	(0.02)	(64)	(10c)	(0.02)	(0.05)	(0.02)	(75)	(318c)	(0.02)
5	0.16	0.02	66	144a		0.07	0.00	63	322a		0.05	0.00	53	279c	
	(0.14)	(0.02)	(78)	(124a)	(0.01)	(0.05)	(0.01)	(60)	(310a)	(0.02)	(0.05)	(0.01)	(60)	(262a)	(0.02)
6	0.08	0.03	146	103c		0.05	0.05	135	11c		0.03	0.03	45	240c	
	(0.07)	(0.03)	(159)	(80c)	(0.05)	(0.04)	(0.03)	(99)	(303c)	(0.02)	(0.03)	(0.02)	(78)	(214c)	(0.03)
7	0.14	0.06	157	102c		0.09	0.06	59	288c		0.06	0.04	68	260c	
	(0.10)	(0.05)	(169)	(95c)	(0.05)	(0.05)	(0.02)	(70)	(287c)	(0.02)	(0.03)	(0.02)	(81)	(239c)	(0.02)
8	0.16	0.09	154	90c		0.07	0.05	77	242c		0.06	0.04	68	212c	
	(0.18)	(0.08)	(150)	(82c)	(0.03)	(0.08)	(0.05)	(76)	(193c)	(0.02)	(0.06)	(0.03)	(53)	(126c)	(0.01)
9	0.11	0.06	147	55c		0.03	0.02	103	354c		0.03	0.02	94	280c	
	(0.12)	(0.06)	(151)	(?)	(0.04)	(0.04)	(0.03)	(10)	(?)	(0.06)	(0.02)	(0.01)	(90)	(?)	(0.03)
10	0.09	0.01	99	81c		0.04	0.02	109	308c		0.03	0.01	95	253c	
	(0.09)	(0.01)	(88)	(?)	(0.04)	(0.04)	(0.00)	(72)	(?)	(0.03)	(0.06)	(0.03)	(69)	(?)	(0.03)

* A - major axis amplitude
B - minor axis amplitude
< - ellipse inclination
P - Greenwich phase lag (c clockwise rotation, a anticlockwise rotation)
± - typical amplitude change over a distance of one model cell
(estimated observational uncertainty)

5. PREDICTION OF TIDAL ELEVATIONS AND CURRENTS

Model results are presented in terms of cotidal charts and tidal ellipses in Appendices A and B, respectively. These may be used to estimate the spatial distribution and timing of tidal elevation and currents over the Scotian Shelf and the Grand Banks. The M2 cotidal charts are in good agreement with earlier charts based on visual interpolation of available observations by Dohler (1966), Godin (1980) and Moody et al. (1984). The diurnal cotidal charts are also in general agreement with earlier charts, with one significant exception. The present results place the amphidromic points in the Laurentian Channel (K1) and near Middle Bank (O1), rather than centered on Sable Island as is traditionally the case.

The results of the model are also available in computer form, from which tidal elevation and current parameters can be obtained for the M2, K1 and O1 constituents, at each model grid cell. From this information one can also infer the S2 and N2 constituents using the parameters presented in Chapter 3. Tidal elevations and currents can then be predicted for any time and location in the study area, using standard techniques (Godin, 1972). Based on the level of agreement between model predictions and observations, we can estimate that the error from such predictions would typically be 5% of the tidal amplitude. In using these estimates one should remember that other factors contribute to variations in water level and currents. In the case of elevation, tides clearly dominate the variability but in extreme conditions the effects of storm surges and wave setup can be considerable. Tides

represent a significant fraction of the current signal, but in the study area the total variance is roughly equally shared between tides, atmospheric forcing and other oceanic variability such as eddies.

6. GENERATING POTENTIAL FOR INTERNAL TIDES

According to Baines (1982), the effect of tidal flow over rough topography for the generation of internal tides is analogous to a vertical body force given by an acceleration:

$$a = - N^2 z \int \vec{Q} \cdot \vec{\nabla} \frac{1}{h} \, dt$$

where $N = \frac{g}{\rho} \frac{d\rho}{dz}$ is the buoyancy frequency,

z is the vertical coordinate,

$\vec{Q}$ is the tidal flux, and

h is the local water depth.

Determining the spatial distribution of this body force can give us some indication of where the generation of internal tides will be most important. The first part of the above expression, $N^2 z$, depends on position in the water column and on the density distribution. The second part, $\int \vec{Q} \cdot \vec{\nabla} \frac{1}{h} \, dt$, however, is entirely specified by bathymetry and barotropic circulation. Given that N^2 can be considered horizontally uniform (this is a good approximation for large portions of the study area), the distribution of $\int \vec{Q} \cdot \vec{\nabla} \frac{1}{h} \, dt$ alone can be used to characterize regions of high internal wave generating potential.

As seen earlier tidal propagation in the study area is mostly linear so that each sinusoidal tidal constituent can be considered separately, with $\int \vec{Q}\cdot\vec{\nabla}\frac{1}{h}$ dt given by $\frac{1}{\omega}\vec{Q}\cdot\vec{\nabla}\frac{1}{h}$, with a 90^{o} phase shift (ω is the tidal frequency). Contours of amplitude for $\frac{1}{\omega}\vec{Q}\cdot\vec{\nabla}\frac{1}{h}$ are presented in Appendix C, for the M2, K1 and O1 constituents. Regions with the highest values are along the shelf break and in general, correspond to areas where high internal wave activity has been observed (Sandstrom and Elliott, personal communication, 1986).

The plots of $\frac{1}{\omega}\vec{Q}\cdot\vec{\nabla}\frac{1}{h}$ show variability on a scale comparable to the model resolution. It can be verified from model results that $\vec{Q}$ varies significantly only on length scales of tens of kilometers so that the main quantity responsible for the small scale variability in F is $\vec{\nabla}\frac{1}{h}$. In order to resolve the finer details of the distribution of internal wave forcing, we can therefore consider $\vec{\nabla}\frac{1}{h}$ with a higher spatial resolution while using Q as determined from the coarser grid hydrodynamic model. This was undertaken for the Gully area (Figure 3) which is of special interest for internal wave activity and where there is considerable spatial variability. The most up-to-date bathymetric soundings for the area were digitized and then used to define water depths on a 2' by 2' grid (approximately 2.6 km by 3.7 km), which corresponds to the highest resolution practically possible with the present data. Model estimates of $\vec{Q}$ defined on the 4' by 4' grid are interpolated on the 2' by 2' grid to compute $\frac{1}{\omega}\vec{Q}\cdot\vec{\nabla}\frac{1}{h}$. High resolution contours of the forcing factor for the Gully area are presented in Appendix D. Given the limited resolution of the bathymetric data over most of the study area, similar calculations are difficult to justify elsewhere.

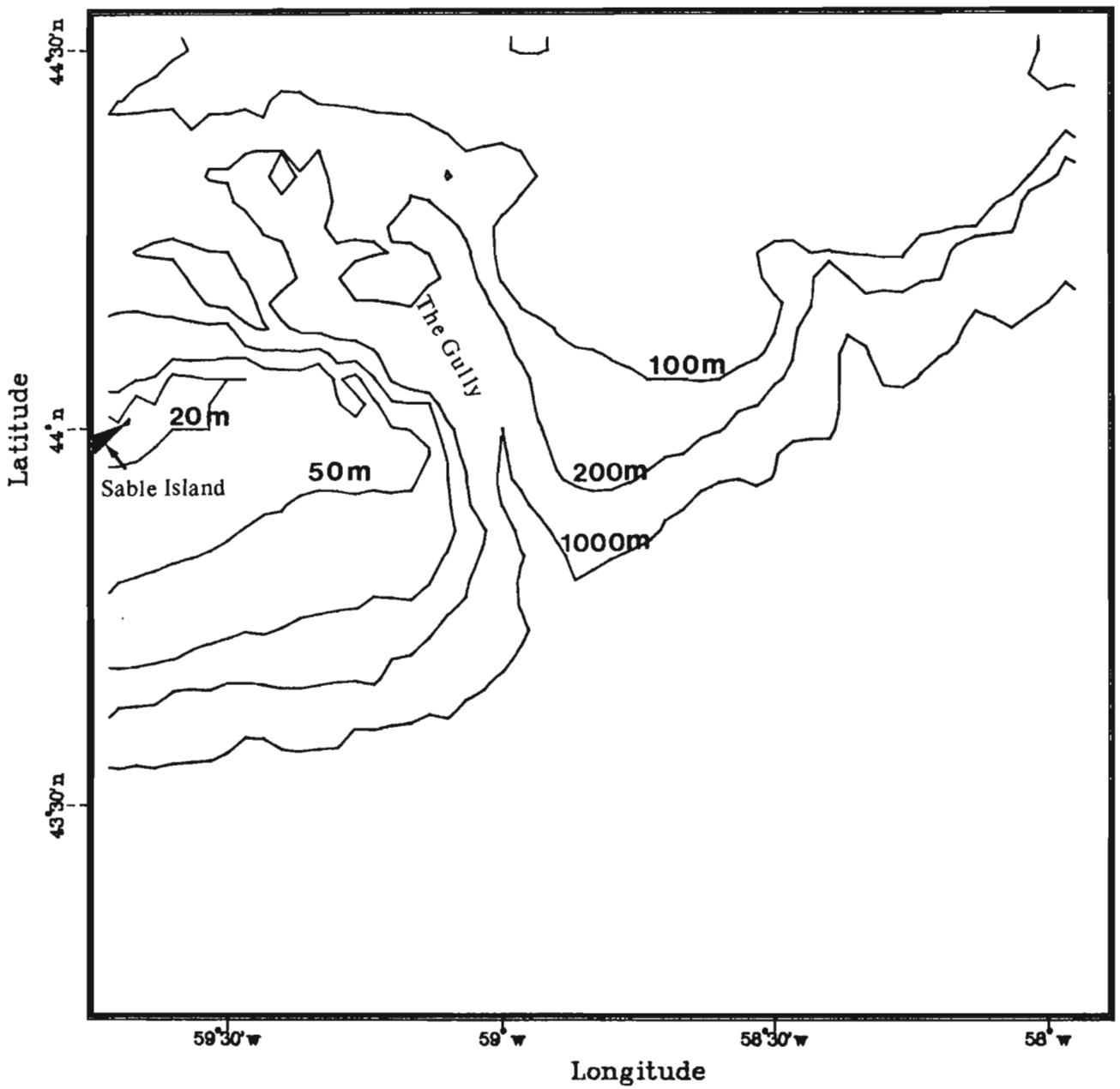

FIGURE 3 Area Used for Detailed Estimates of Internal Tide Forcing.

REFERENCES

Baines, P.G., 1982, "On Internal Tide Generation Models", Deep Sea Res., Vol 29, p. 307-338.

de Margerie, S., 1985, "Barotropic Tidal Circulation of the Scotian Shelf", contract report to the Canadian Hydrographic Service, contract no. OSC84-00218.

Dohler, A.M., 1966, "Tides in Canadian Waters", Canadian Hydrographic Service, Marine Sciences Branch, Dept. of Marine and Technical Surveys, Ottawa, Canada, 16p.

Godin, G., 1972, "The Analysis of Tides", University of Toronto Press, 264p.

Godin, G., 1980, "Cotidal Charts for Canada", Marine Science and Information Directorate, Department of Fisheries and Oceans, Ottawa, Canada, 93p.

Greenberg, D., 1983, "Modeling the Mean Barotropic Circulation in the Bay of Fundy and Gulf of Maine", Jour. Phys. Ocean., Vol. 13, No. 5, p. 886-904.

Petrie, B., 1982, "Aspects of the Circulation on the Newfoundland Continental Shelf", Canadian Technical Report of Hydrography and Ocean Sciences, No. 11, 78p.

Moody, J. et al., 1984, "Atlas of Tidal Elevations and Current Observations on the Northeast American Continental Shelf and Slope", US Geological Survey, Bulletin No 1611.

Rattray, M., Jr., 1960, "On the Coastal Generation of Internal Tides", Tellus, Vol 12, No 54.

Sandstrom, H. and J.A. Elliott, 1984, "Internal Tide and Solitons on the Scotian Shelf: a Nutrient Pump at Work", Jour. Geophys. Res., Vol 89, No C4, p. 6415-6426.

Smith, P., 1983, "The Mean and Seasonal Circulation off Southwest Nova Scotia", Jour. Phys. Ocean. Vol 13, No 6, p. 1034-1054.

Smith, P.C., B. Petrie and C.R. Mann, 1978, "Circulation, Variability, and Dynamics of the Scotian Shelf and Slope", Jour. Fish. Res. Board Can, Vol 35, p. 1067-1083.

Wunsch, C., 1975, "Internal Tides in the Ocean", review of Geophysical Space Physics, Vol 13, No 1, p. 167-182.

APPENDIX A
Cotidal Charts for the Scotian Shelf and the Grand Banks

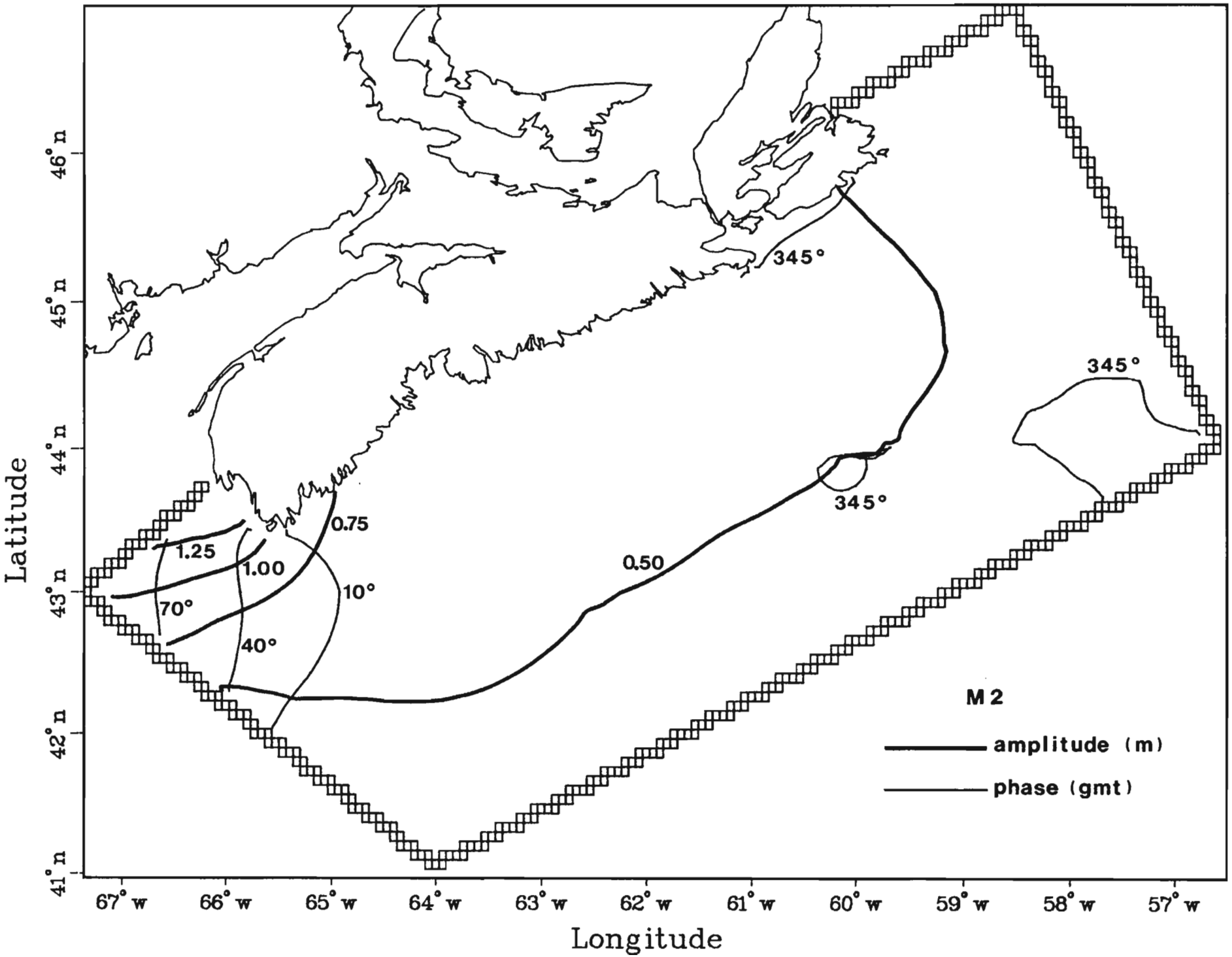
46° n
45° n
44° n
43° n
42° n
41° n
67° w
66° w
65° w
64° w
63° w
62° w
61° w
60° w
59° w
58° w
57° w
Latitude
Longitude
345°
345°
345°
0.75
1.25
1.00
0.50
10°
70°
40°
M 2
amplitude (m)
phase (gmt)

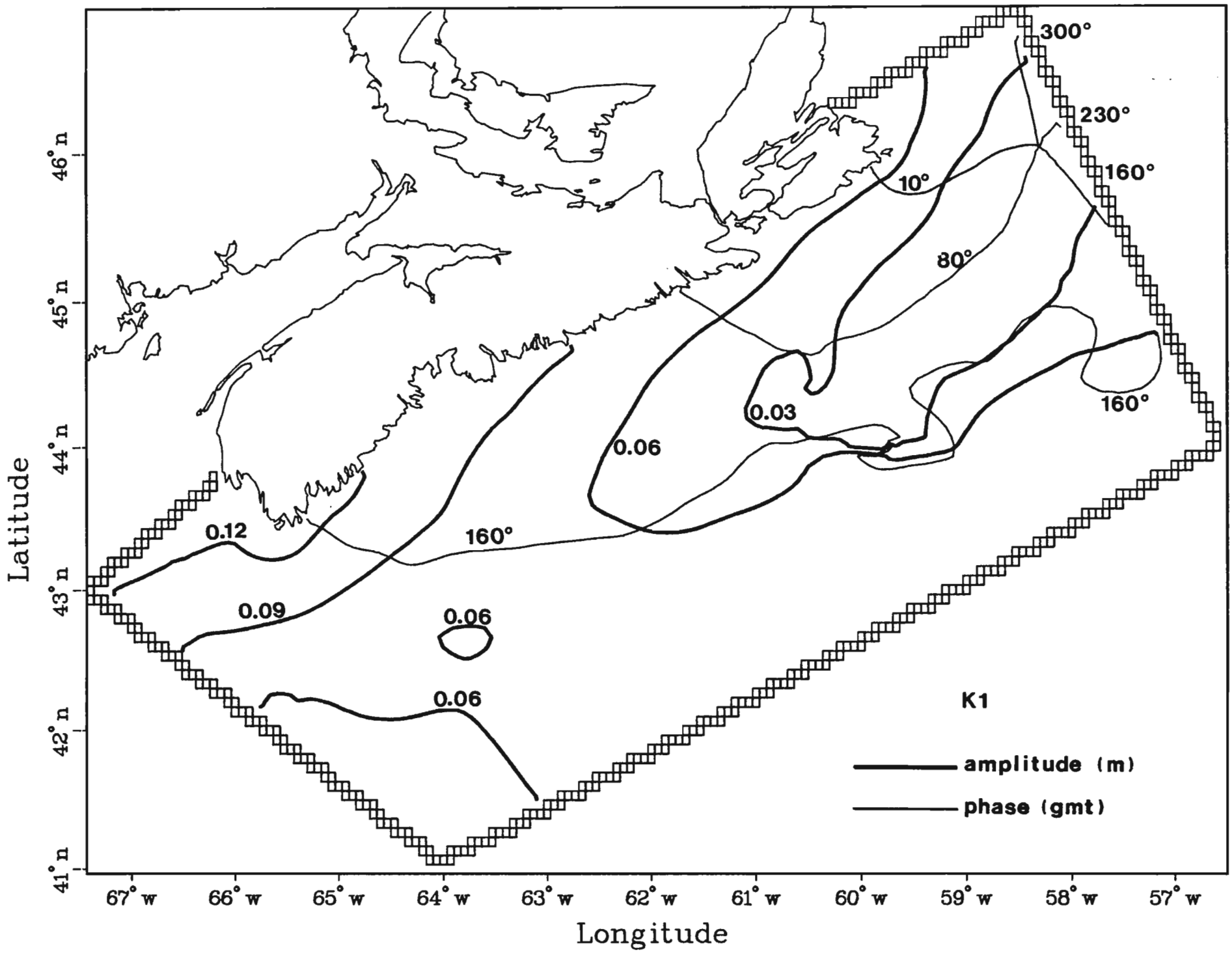
300°
230°
160°
10°
80°
160°
0.03
0.06
0.12
160°
0.09
0.06
0.06
K1
amplitude (m)
phase (gmt)
46° n
45° n
44° n
43° n
42° n
41° n
67° w
66° w
65° w
64° w
63° w
62° w
61° w
60° w
59° w
58° w
57° w
Latitude
Longitude

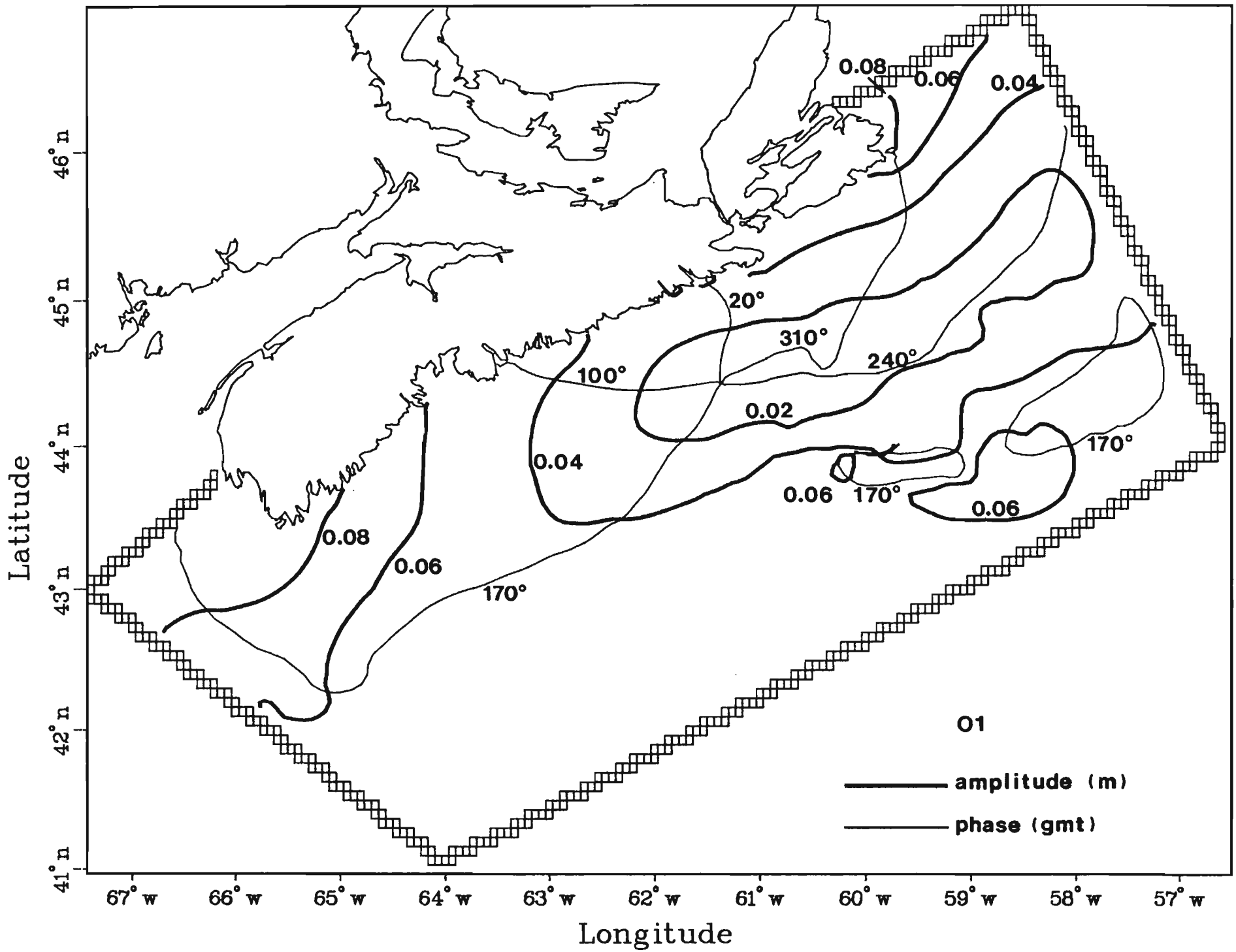
0.08
0.06
0.04
20°
310°
240°
100°
0.02
0.04
170°
0.06
170°
0.06
0.08
0.06
170°
O1
amplitude (m)
phase (gmt)
46° n
45° n
44° n
43° n
42° n
41° n
67° w
66° w
65° w
64° w
63° w
62° w
61° w
60° w
59° w
58° w
57° w
Latitude
Longitude

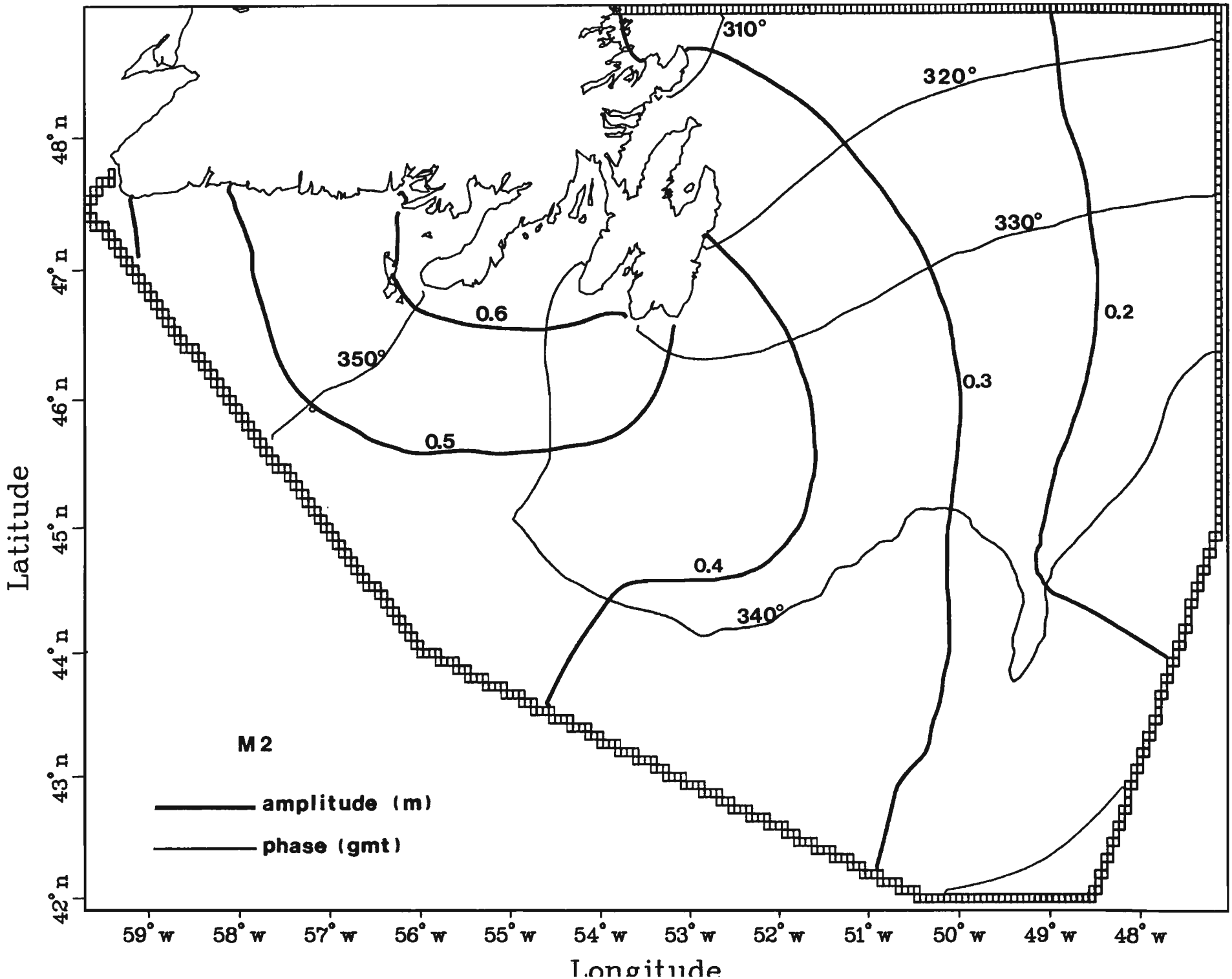
310°
320°
330°
350°
0.6
0.5
0.4
0.3
0.2
340°
M2
amplitude (m)
phase (gmt)
Latitude
Longitude
48° n
47° n
46° n
45° n
44° n
43° n
42° n
59° w
58° w
57° w
56° w
55° w
54° w
53° w
52° w
51° w
50° w
49° w
48° w

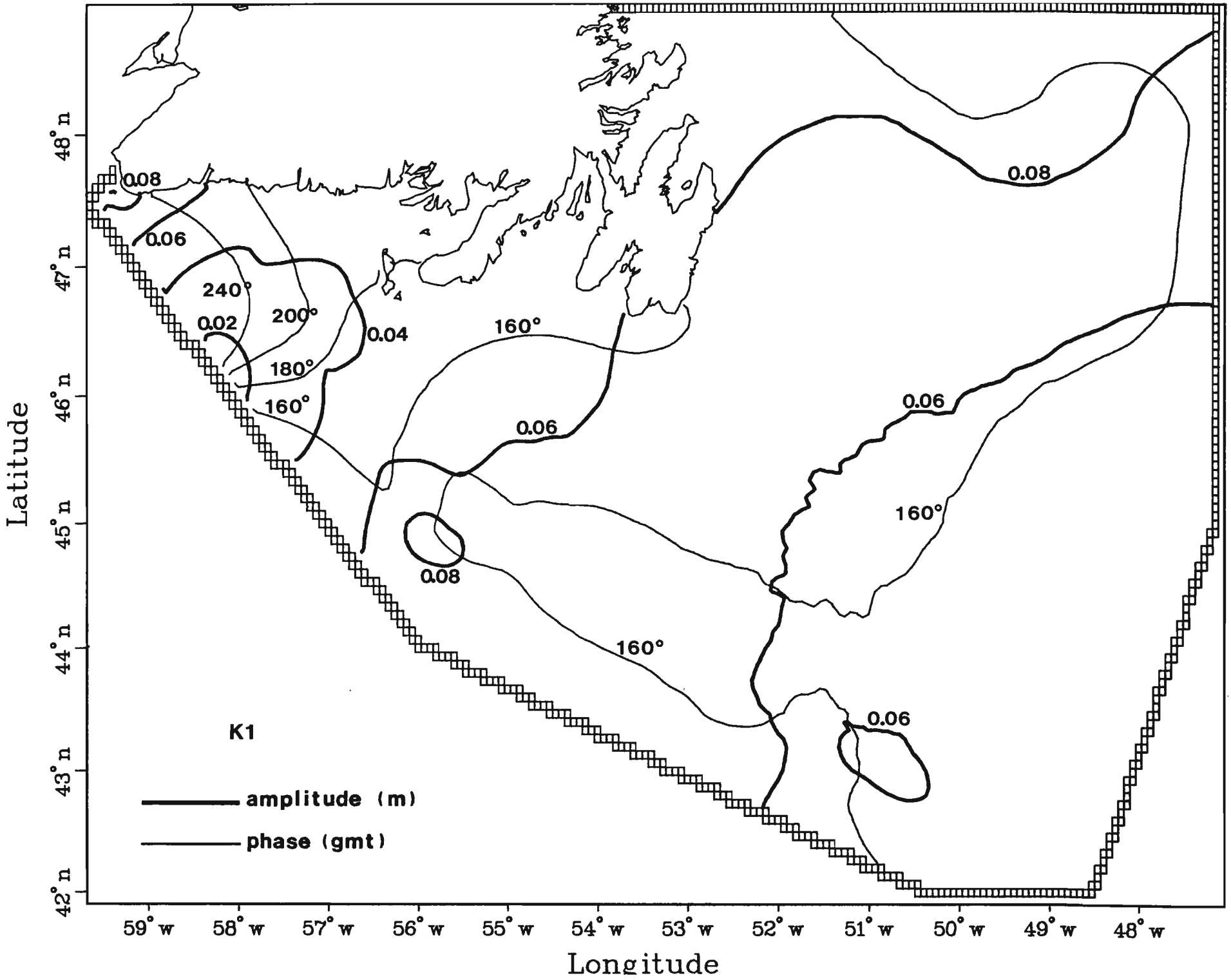
0.08
0.06
240°
200°
0.02
0.04
180°
160°
160°
0.06
0.08
0.06
160°
0.08
160°
0.06
K1
amplitude (m)
phase (gmt)
48° n
47° n
46° n
45° n
44° n
43° n
42° n
59° w
58° w
57° w
56° w
55° w
54° w
53° w
52° w
51° w
50° w
49° w
48° w
Latitude
Longitude

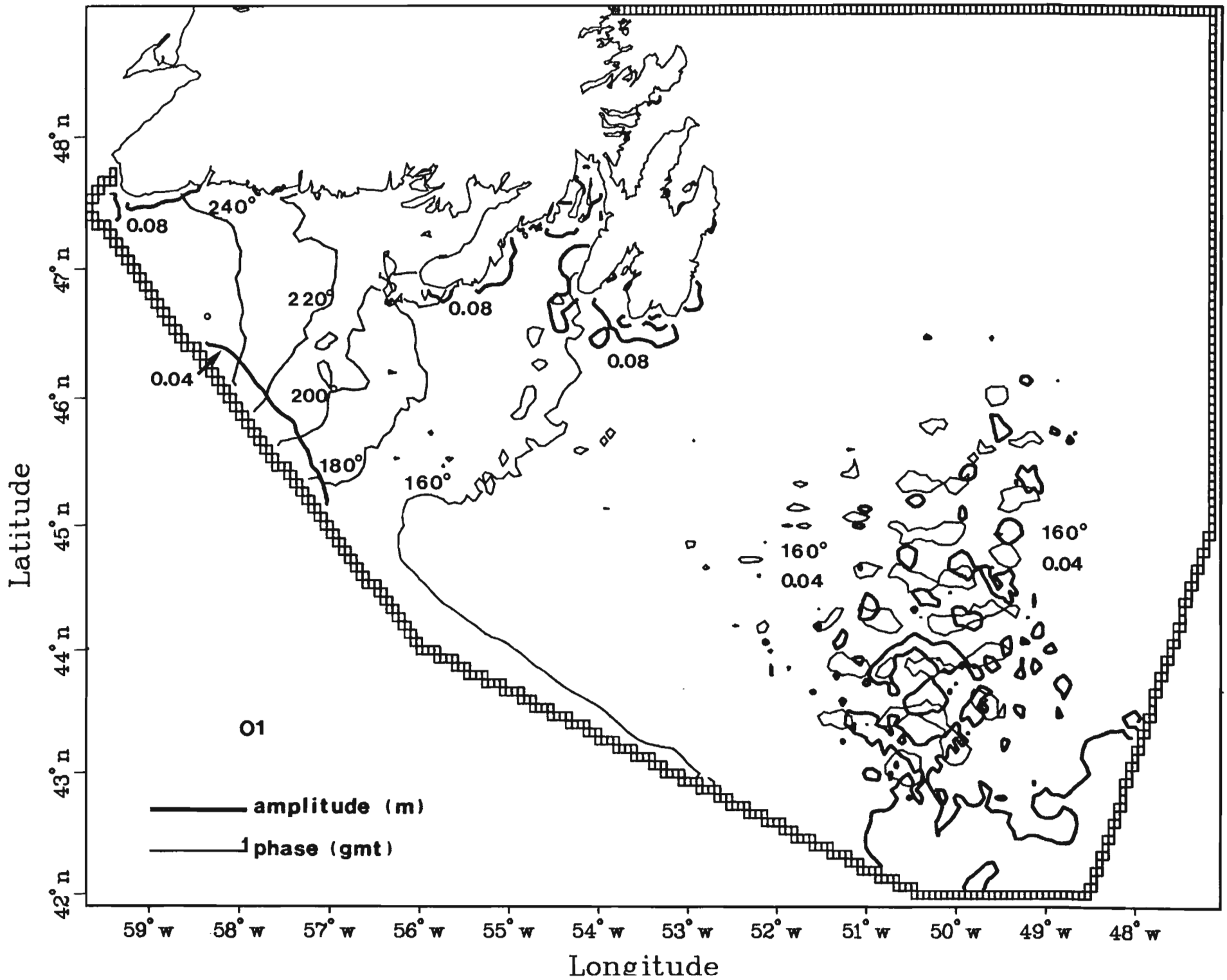
Latitude
Longitude
48° n
47° n
46° n
45° n
44° n
43° n
42° n
59° w
58° w
57° w
56° w
55° w
54° w
53° w
52° w
51° w
50° w
49° w
48° w
240°
0.08
220°
0.08
0.08
0.04
200°
180°
160°
160°
0.04
160°
0.04
O1
amplitude (m)
phase (gmt)

APPENDIX B
Tidal Ellipses for the Scotian Shelf and the Grand Banks

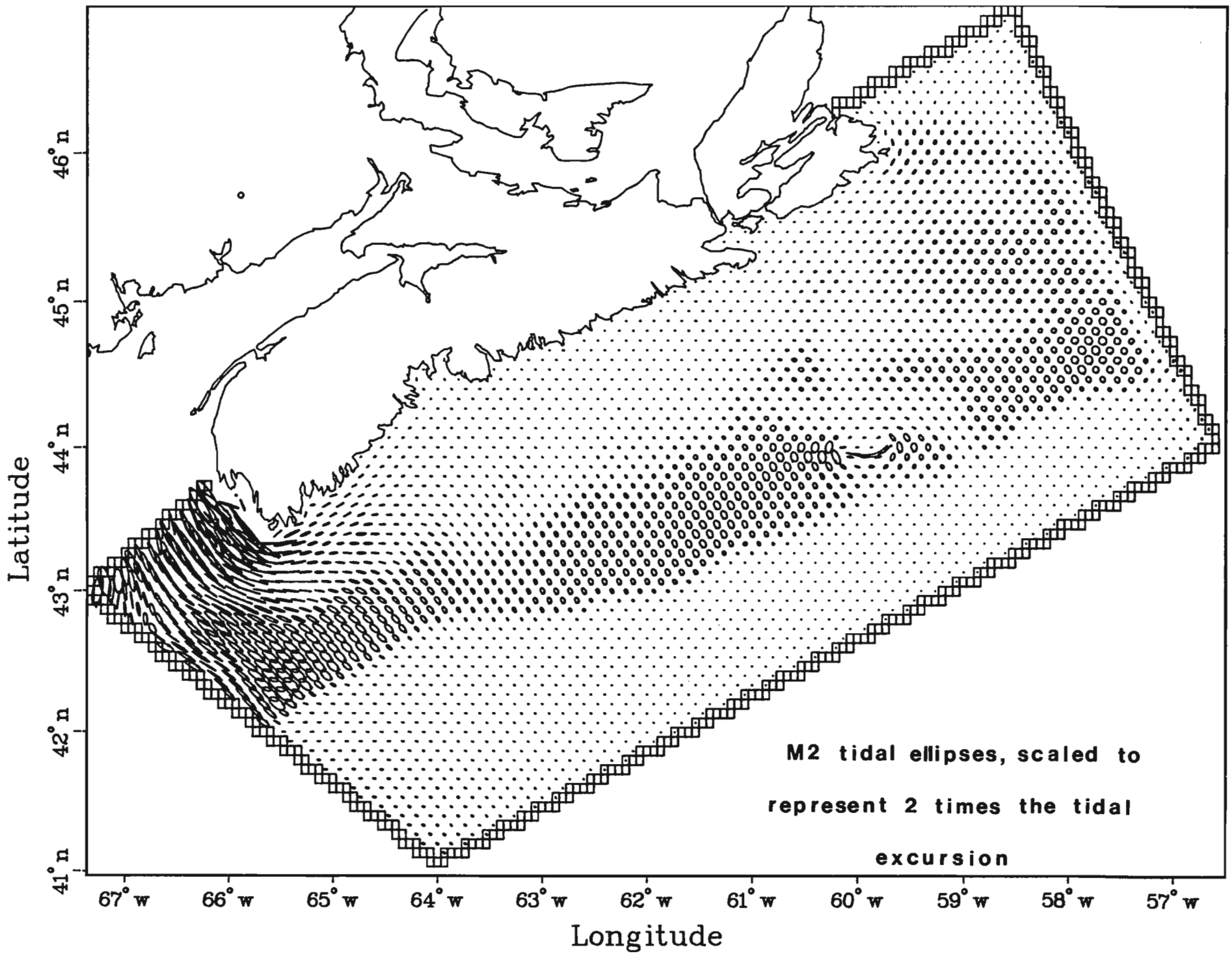
Latitude
46° n
45° n
44° n
43° n
42° n
41° n
67° w
66° w
65° w
64° w
63° w
62° w
61° w
60° w
59° w
58° w
57° w
Longitude
M2 tidal ellipses, scaled to represent 2 times the tidal excursion

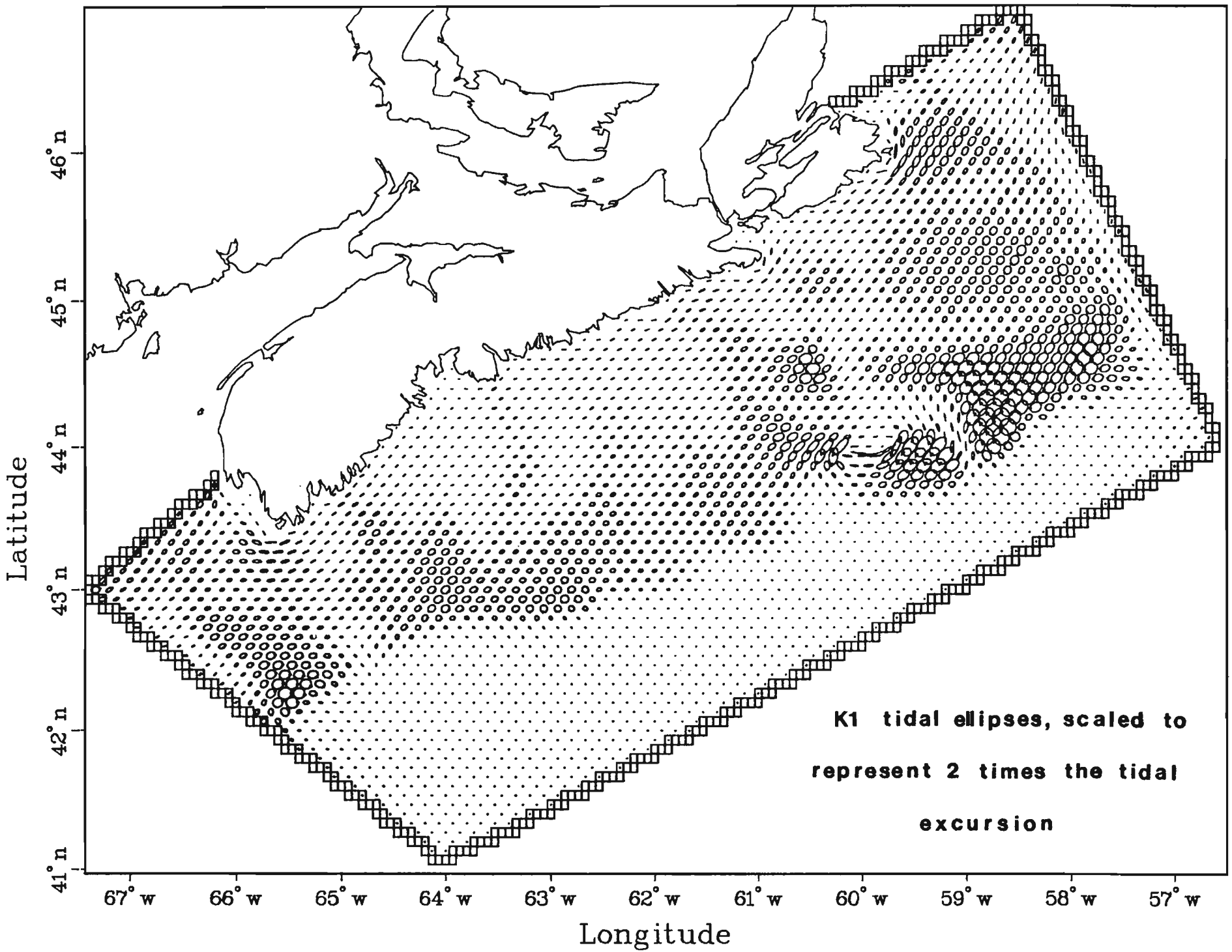
K1 tidal ellipses, scaled to represent 2 times the tidal excursion
Latitude
46° n
45° n
44° n
43° n
42° n
41° n
67° w
66° w
65° w
64° w
63° w
62° w
61° w
60° w
59° w
58° w
57° w
Longitude

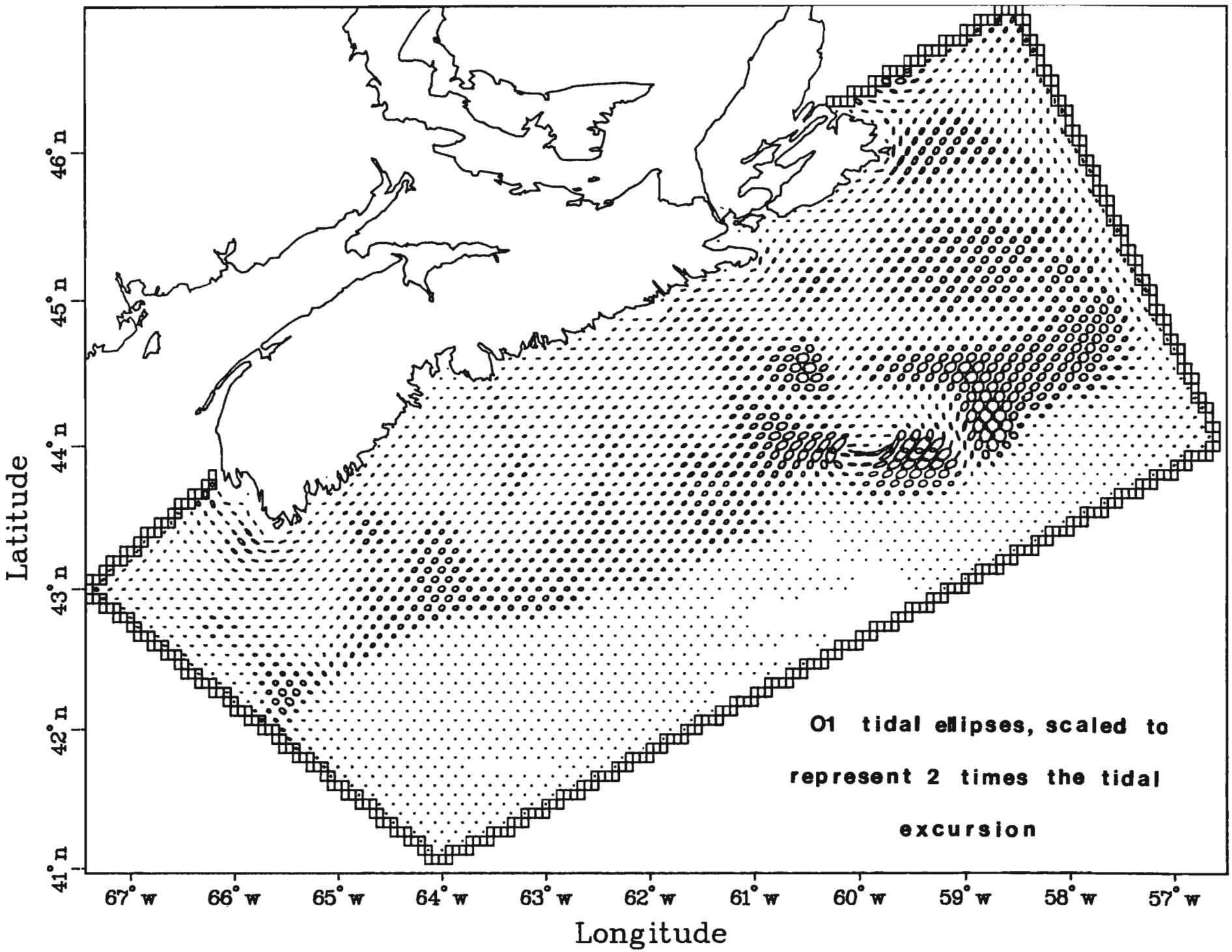
O1 tidal ellipses, scaled to represent 2 times the tidal excursion
Latitude
46° n
45° n
44° n
43° n
42° n
41° n
67° w
66° w
65° w
64° w
63° w
62° w
61° w
60° w
59° w
58° w
57° w
Longitude

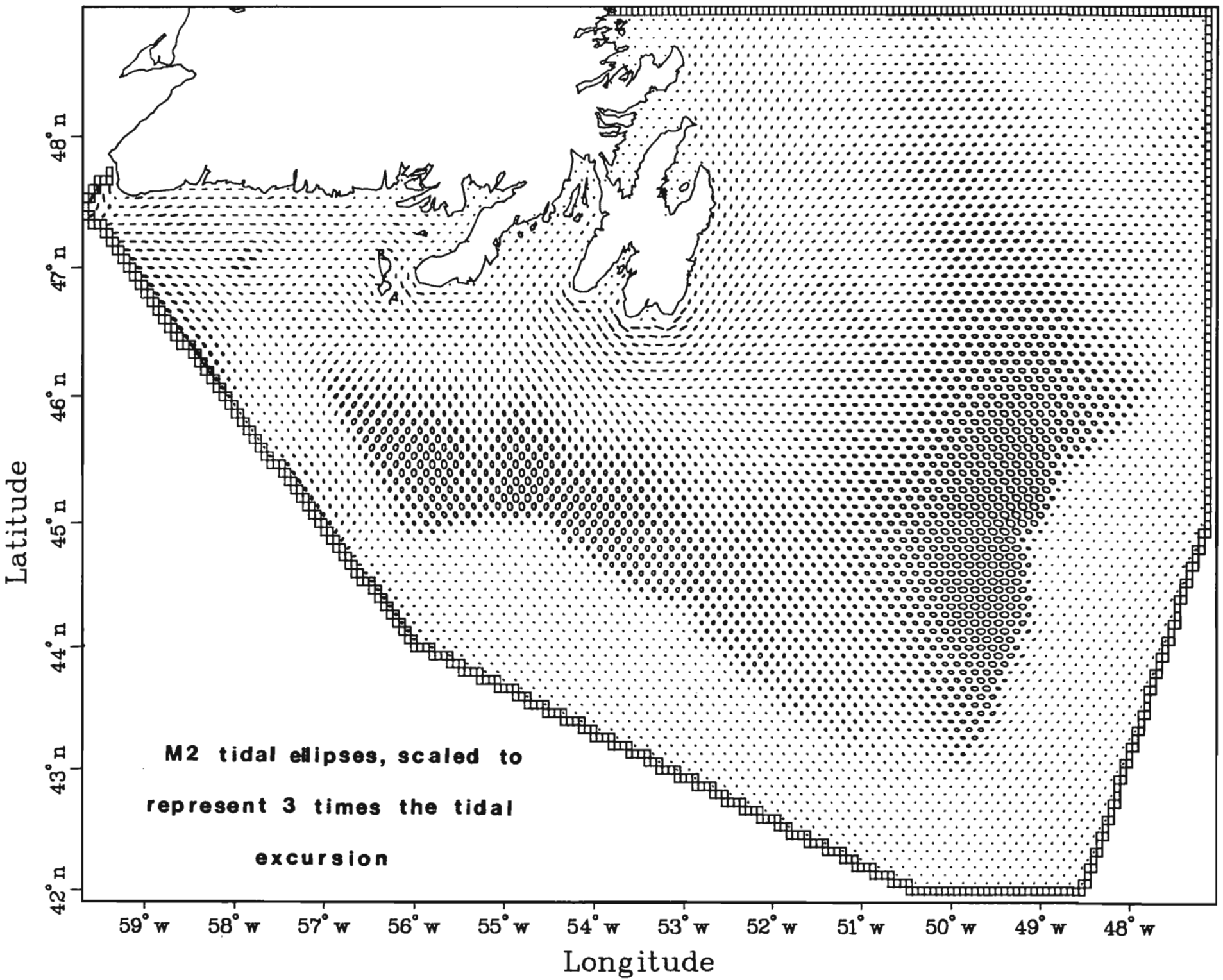
M2 tidal ellipses, scaled to
represent 3 times the tidal
excursion
Latitude
48° n
47° n
46° n
45° n
44° n
43° n
42° n
59° w
58° w
57° w
56° w
55° w
54° w
53° w
52° w
51° w
50° w
49° w
48° w
Longitude

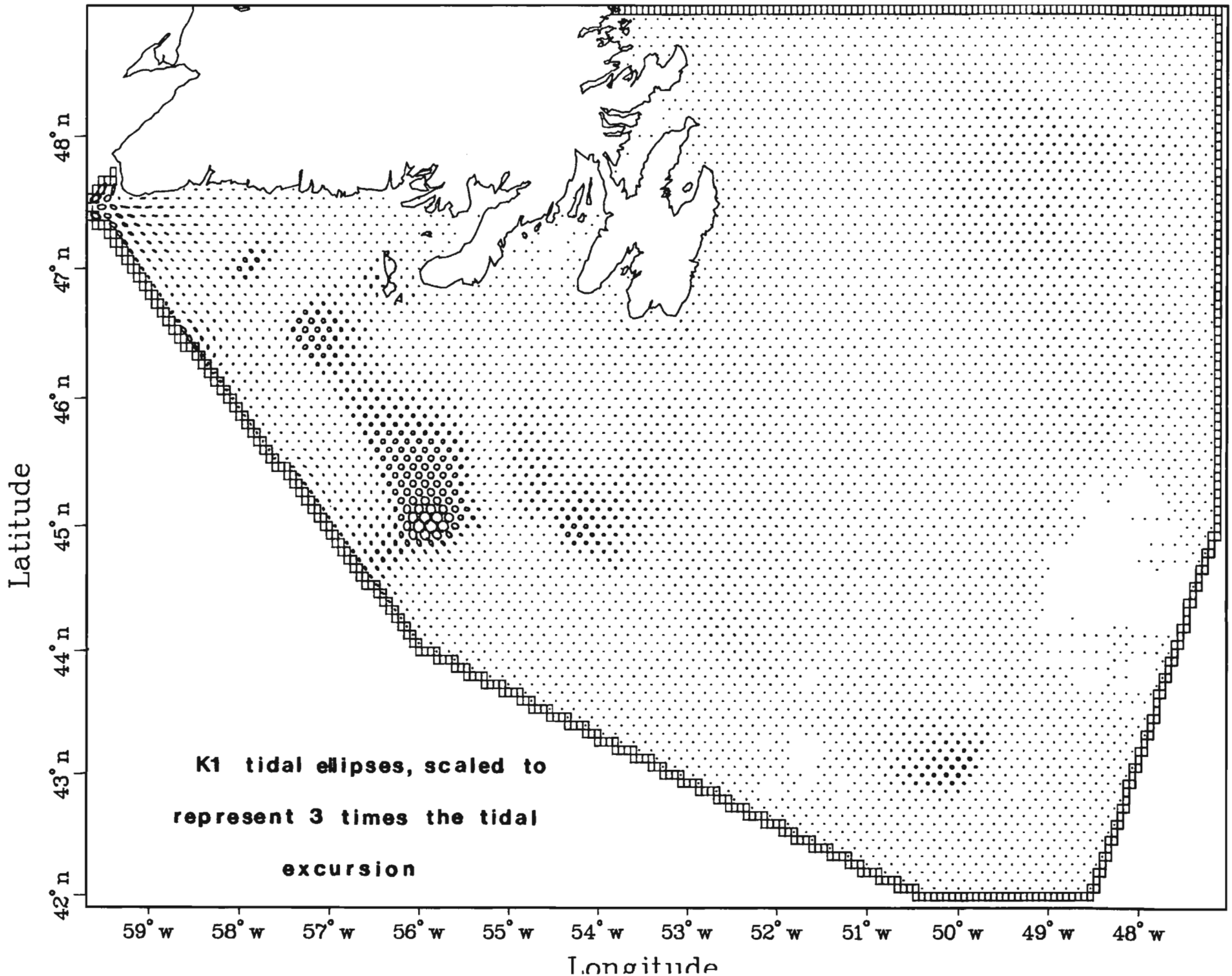
K1 tidal ellipses, scaled to
represent 3 times the tidal
excursion
Latitude
48° n
47° n
46° n
45° n
44° n
43° n
42° n
59° w
58° w
57° w
56° w
55° w
54° w
53° w
52° w
51° w
50° w
49° w
48° w
Longitude

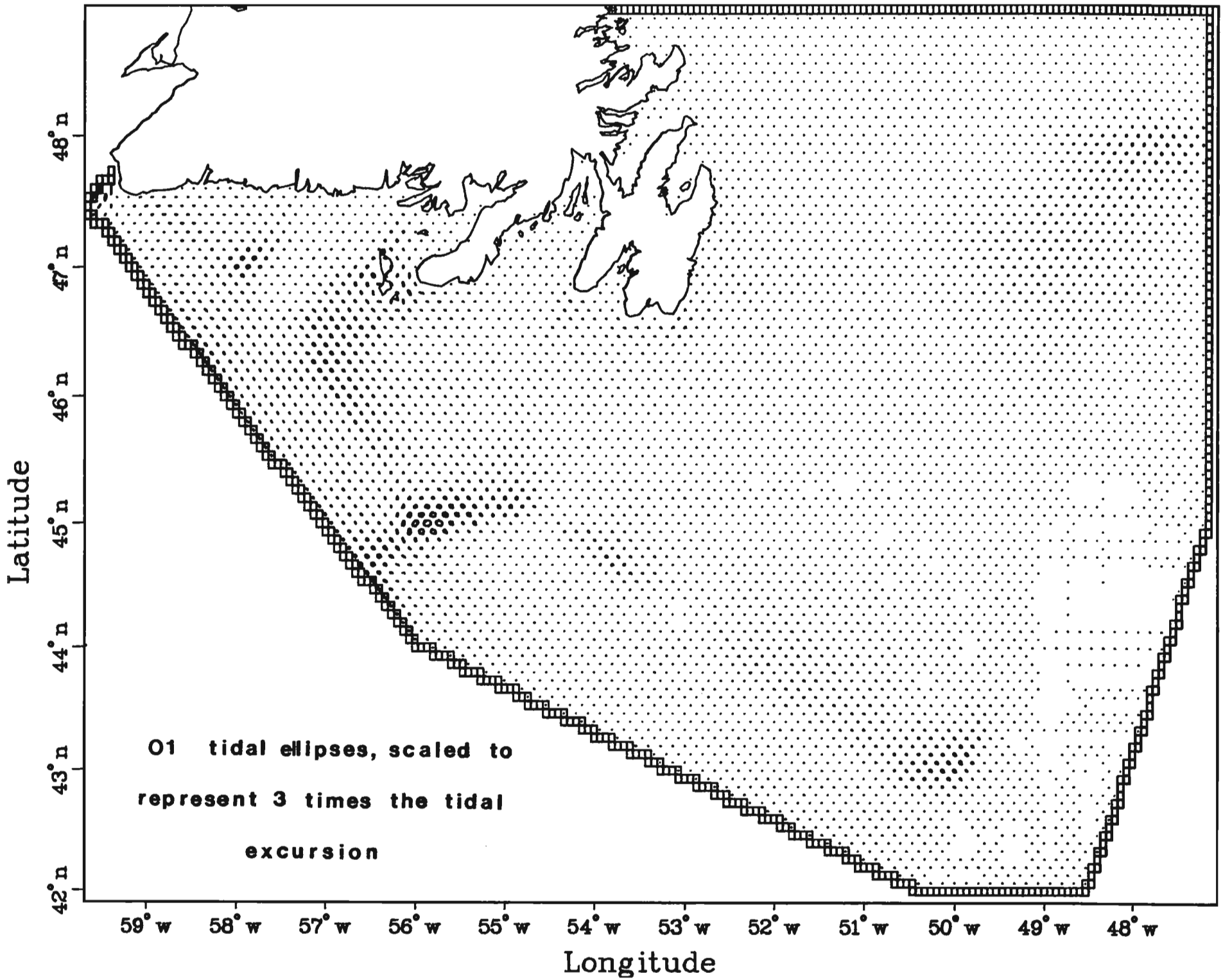
O1 tidal ellipses, scaled to represent 3 times the tidal excursion
Latitude
48°n
47°n
46°n
45°n
44°n
43°n
42°n
59°w
58°w
57°w
56°w
55°w
54°w
53°w
52°w
51°w
50°w
49°w
48°w
Longitude

APPENDIX C
Internal Tide Forcing for the Scotian Shelf and the Grand Banks

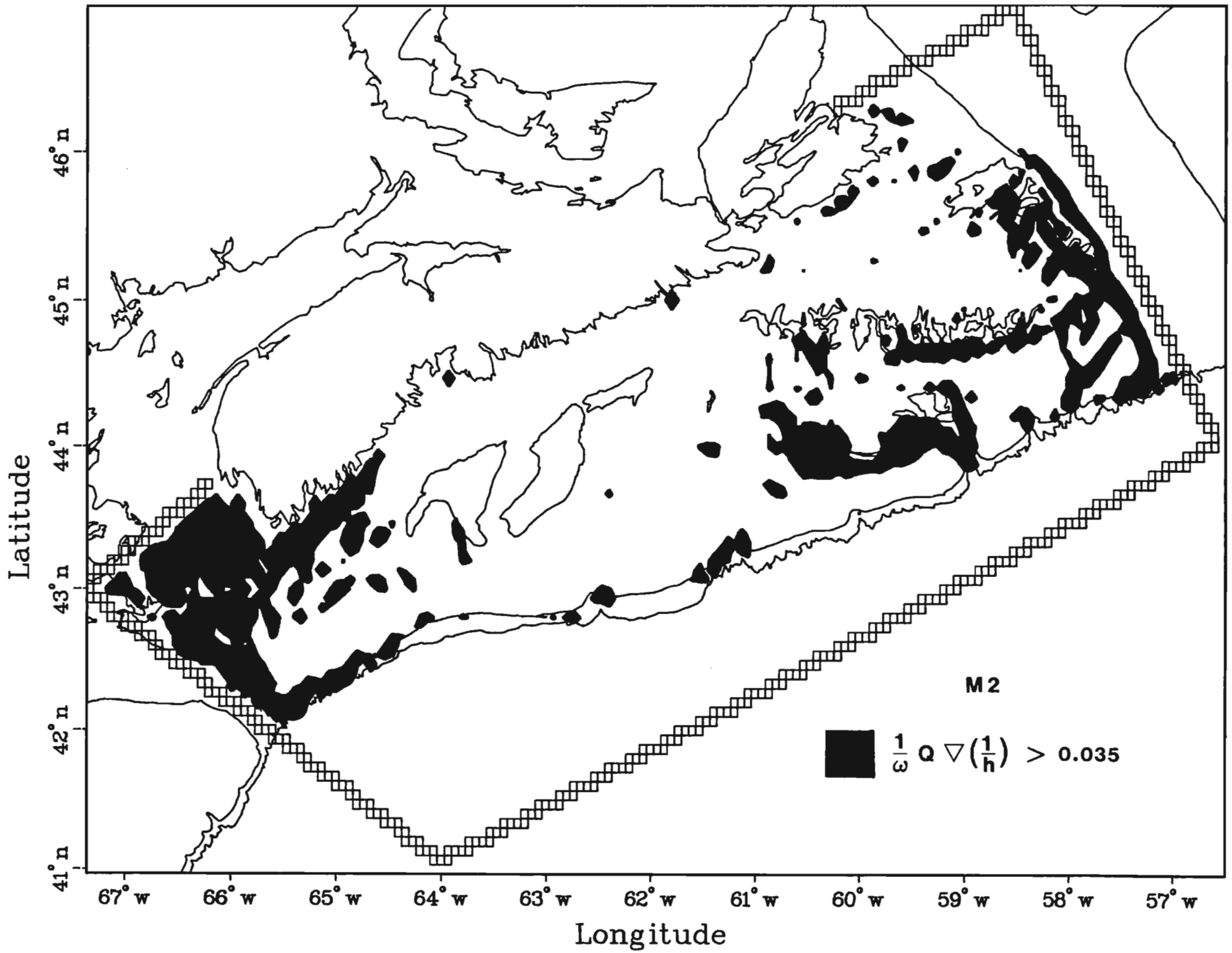
46° n
45° n
44° n
43° n
42° n
41° n
Latitude
67° w
66° w
65° w
64° w
63° w
62° w
61° w
60° w
59° w
58° w
57° w
Longitude
M2
$\frac{1}{\omega} Q \nabla\left(\frac{1}{h}\right) > 0.035$

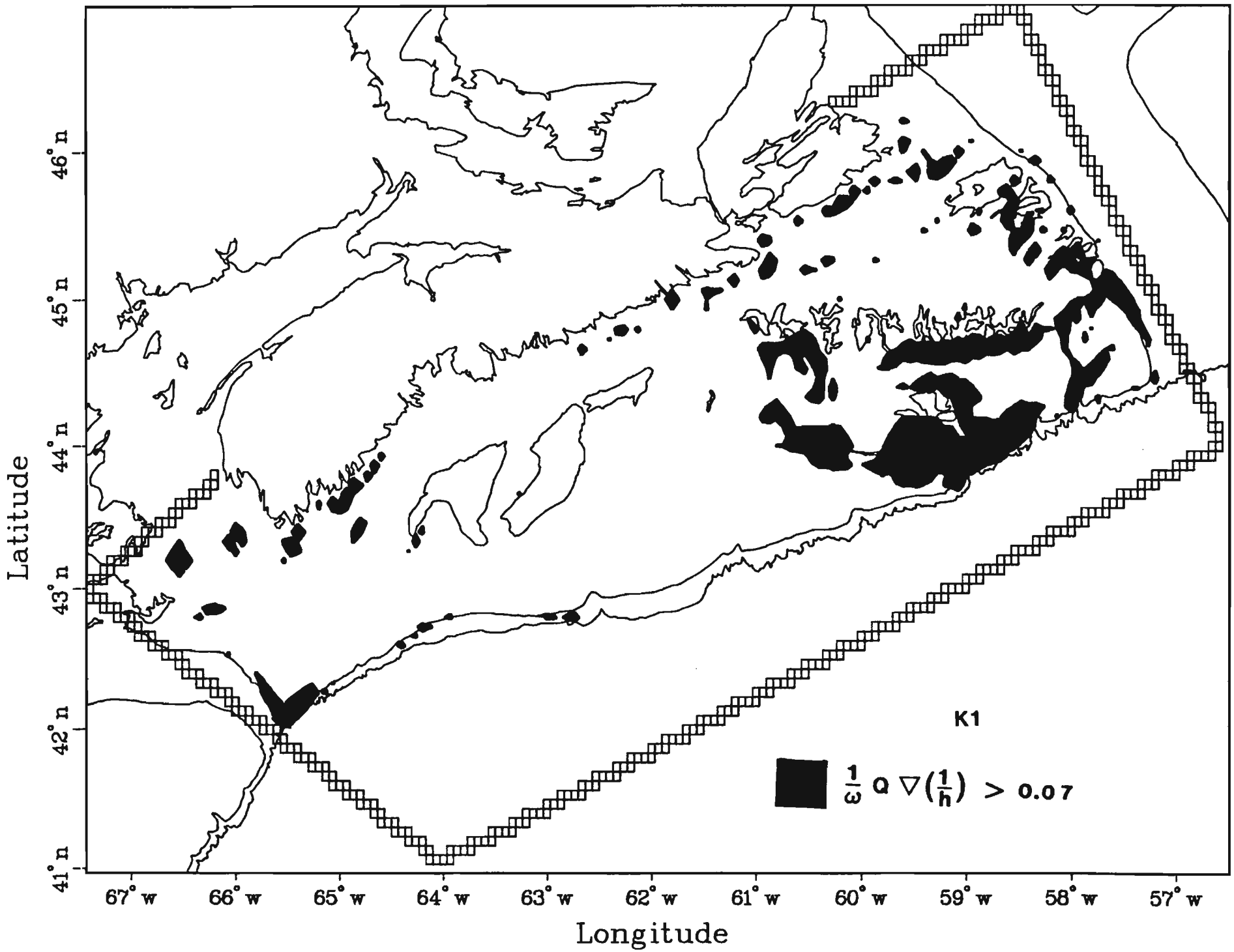
46° n
45° n
44° n
43° n
42° n
41° n
Latitude
67° w
66° w
65° w
64° w
63° w
62° w
61° w
60° w
59° w
58° w
57° w
Longitude
K1
$\frac{1}{\omega} Q \nabla\left(\frac{1}{h}\right) > 0.07$

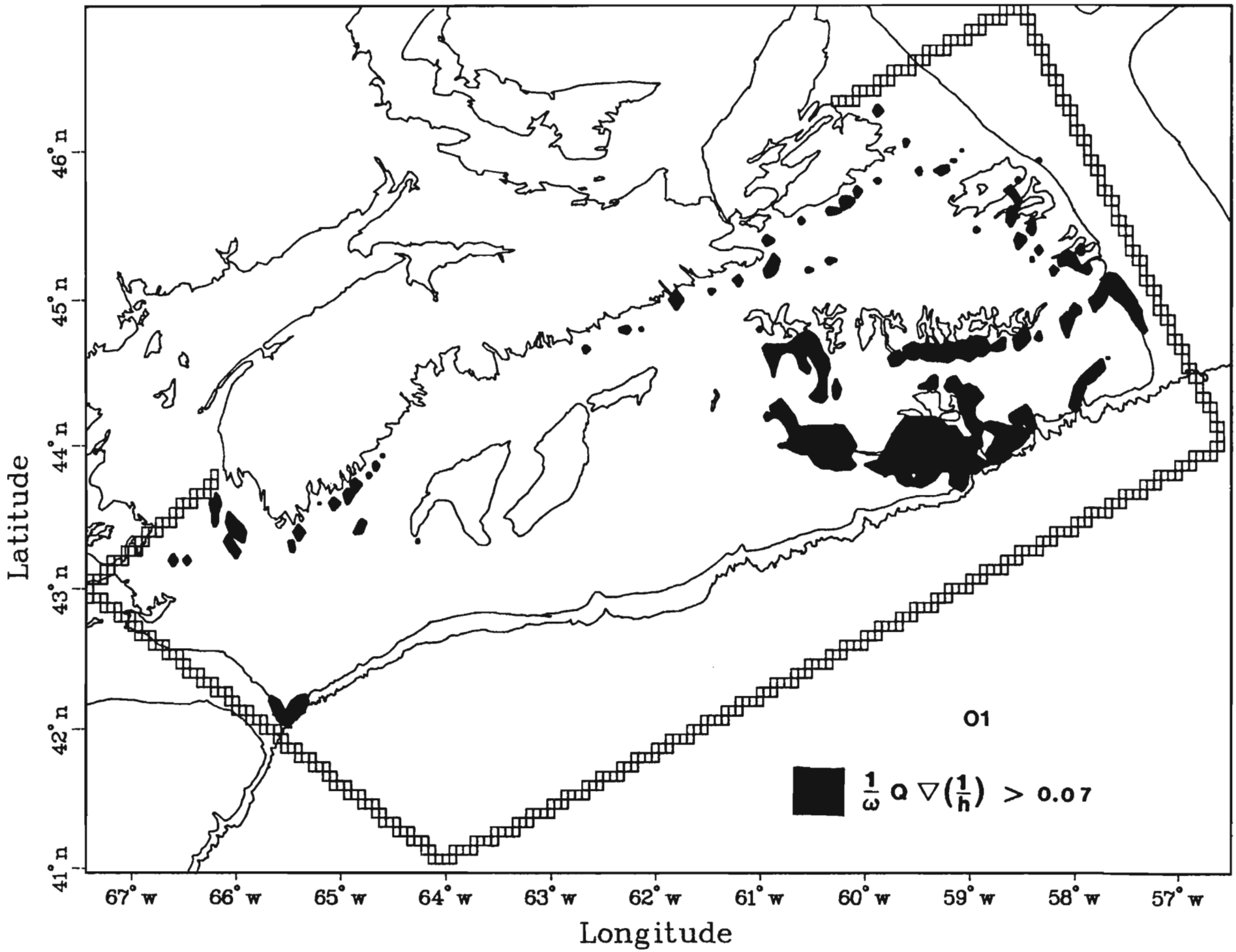
46° n
45° n
44° n
43° n
42° n
41° n
Latitude
67° w
66° w
65° w
64° w
63° w
62° w
61° w
60° w
59° w
58° w
57° w
Longitude
O1
$\frac{1}{\omega} Q \nabla\left(\frac{1}{h}\right) > 0.07$

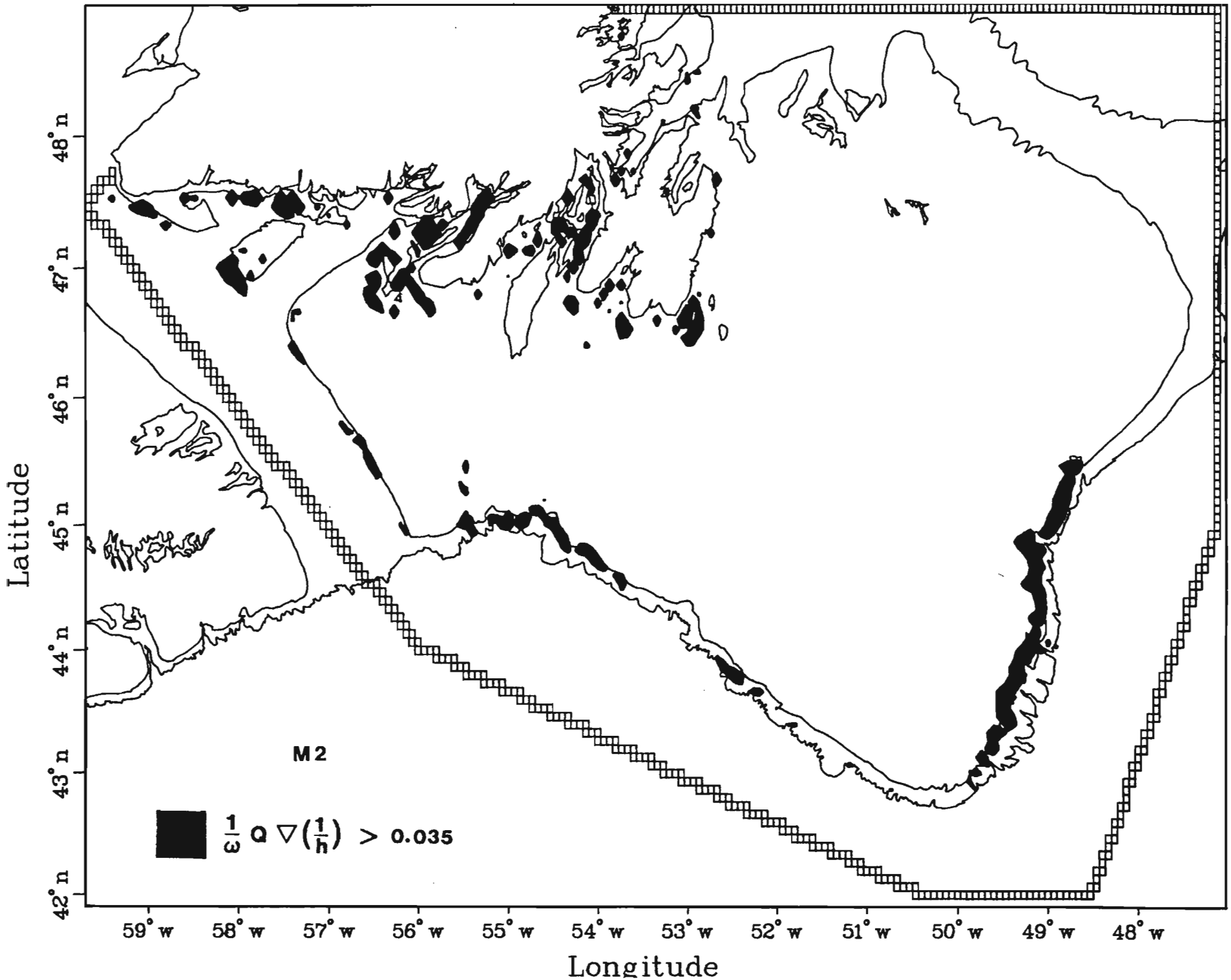
Latitude
48° n
47° n
46° n
45° n
44° n
43° n
42° n
59° w
58° w
57° w
56° w
55° w
54° w
53° w
52° w
51° w
50° w
49° w
48° w
Longitude
M2
$\frac{1}{\omega} Q \nabla\left(\frac{1}{h}\right) > 0.035$

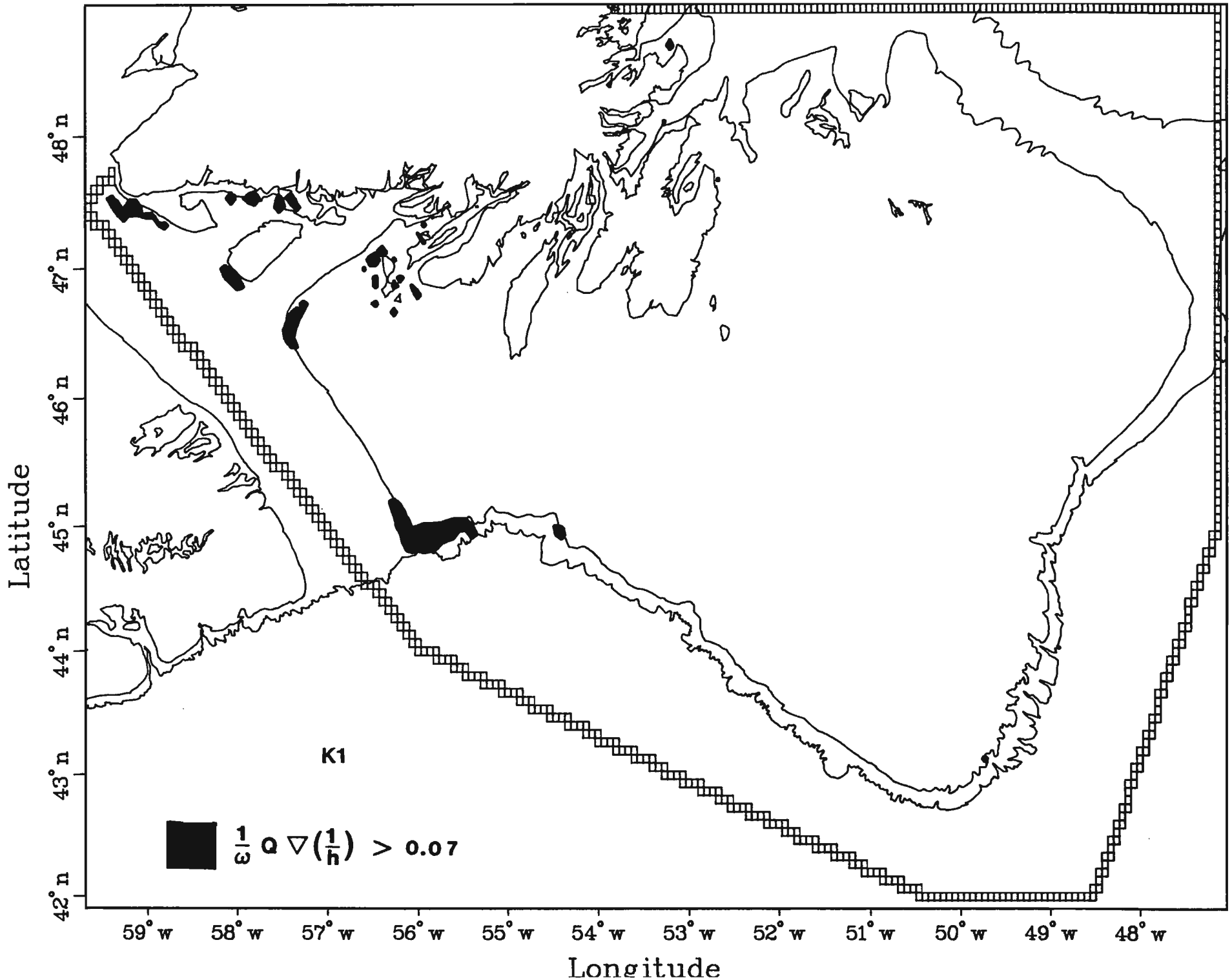
Latitude
48° n
47° n
46° n
45° n
44° n
43° n
42° n
59° w
58° w
57° w
56° w
55° w
54° w
53° w
52° w
51° w
50° w
49° w
48° w
Longitude
K1
$\frac{1}{\varepsilon} Q \nabla\left(\frac{1}{h}\right) > 0.07$

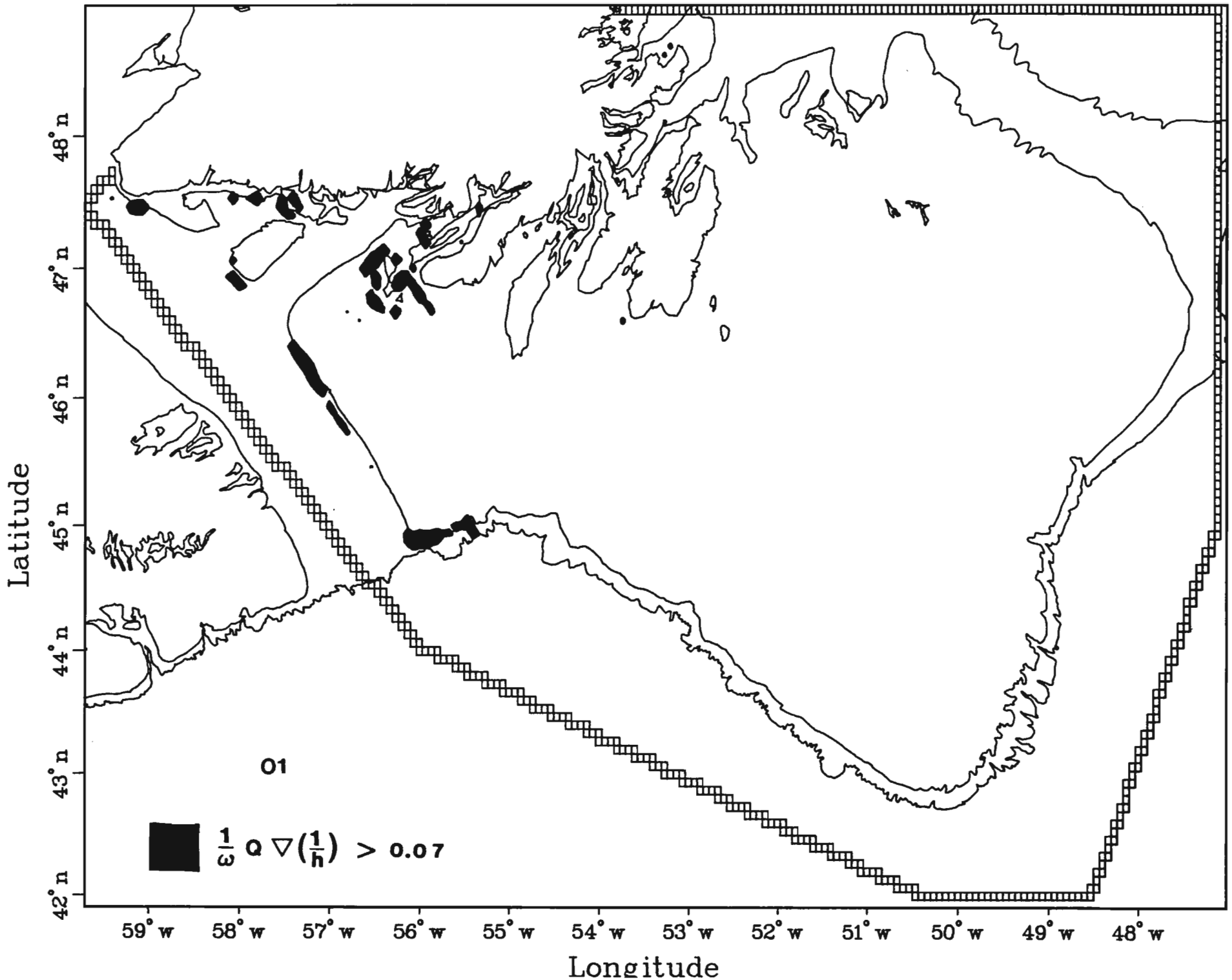
Latitude
48° n
47° n
46° n
45° n
44° n
43° n
42° n
59° w
58° w
57° w
56° w
55° w
54° w
53° w
52° w
51° w
50° w
49° w
48° w
Longitude
01
$\frac{1}{\varepsilon} Q \nabla\left(\frac{1}{h}\right) > 0.07$

APPENDIX D
Details of Internal Tide Forcing for the Gully Area

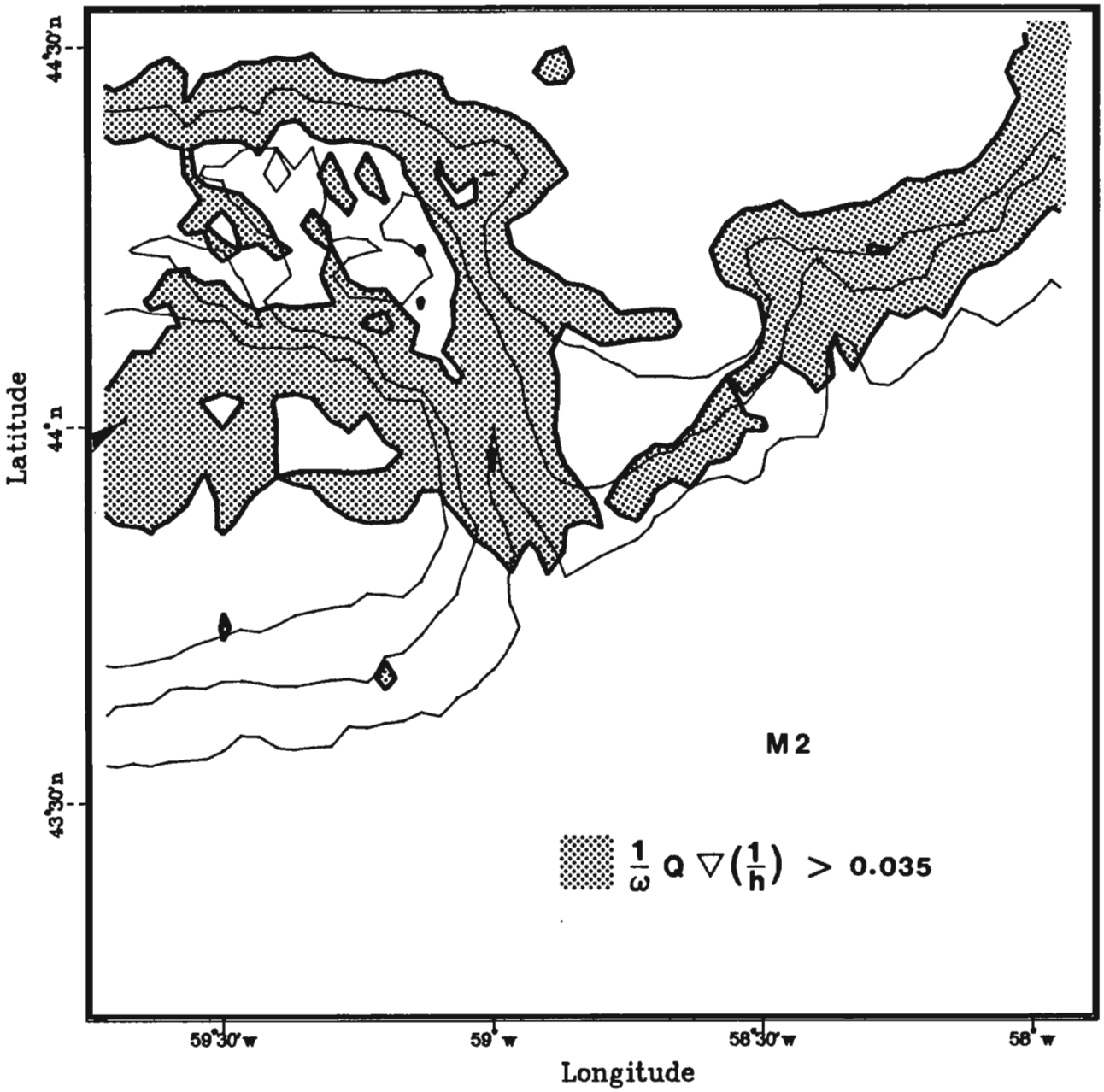
44°30'n
44°n
43°30'n
Latitude
59°30'w
59°w
58°30'w
58°w
Longitude
M2
$\frac{1}{\omega} Q \nabla\left(\frac{1}{h}\right) > 0.035$

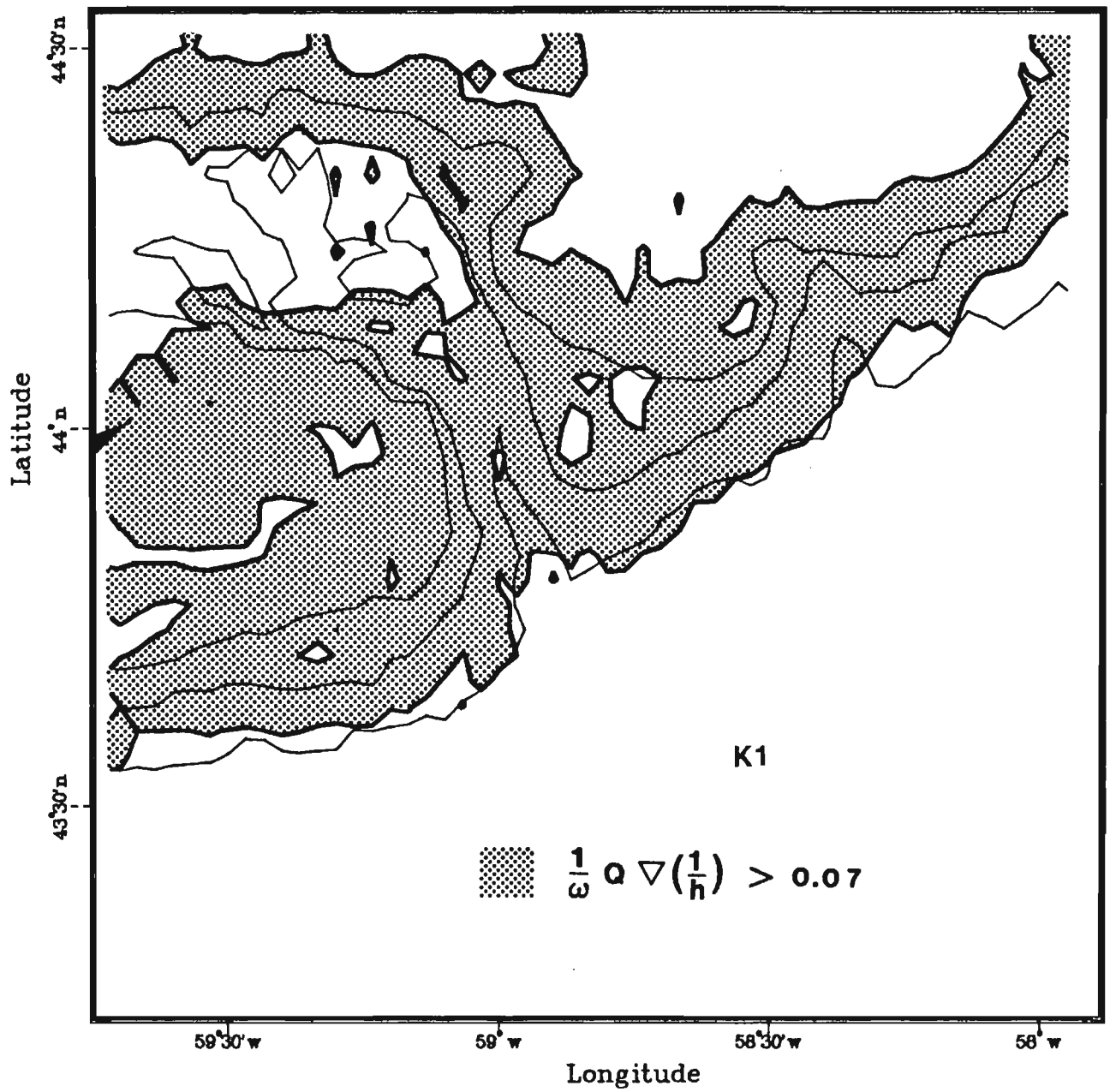
44°30'n
44°n
43°30'n
Latitude
K1
$\frac{1}{\omega} Q \nabla\left(\frac{1}{h}\right) > 0.07$
59°30'w
59°w
58°30'w
58°w
Longitude

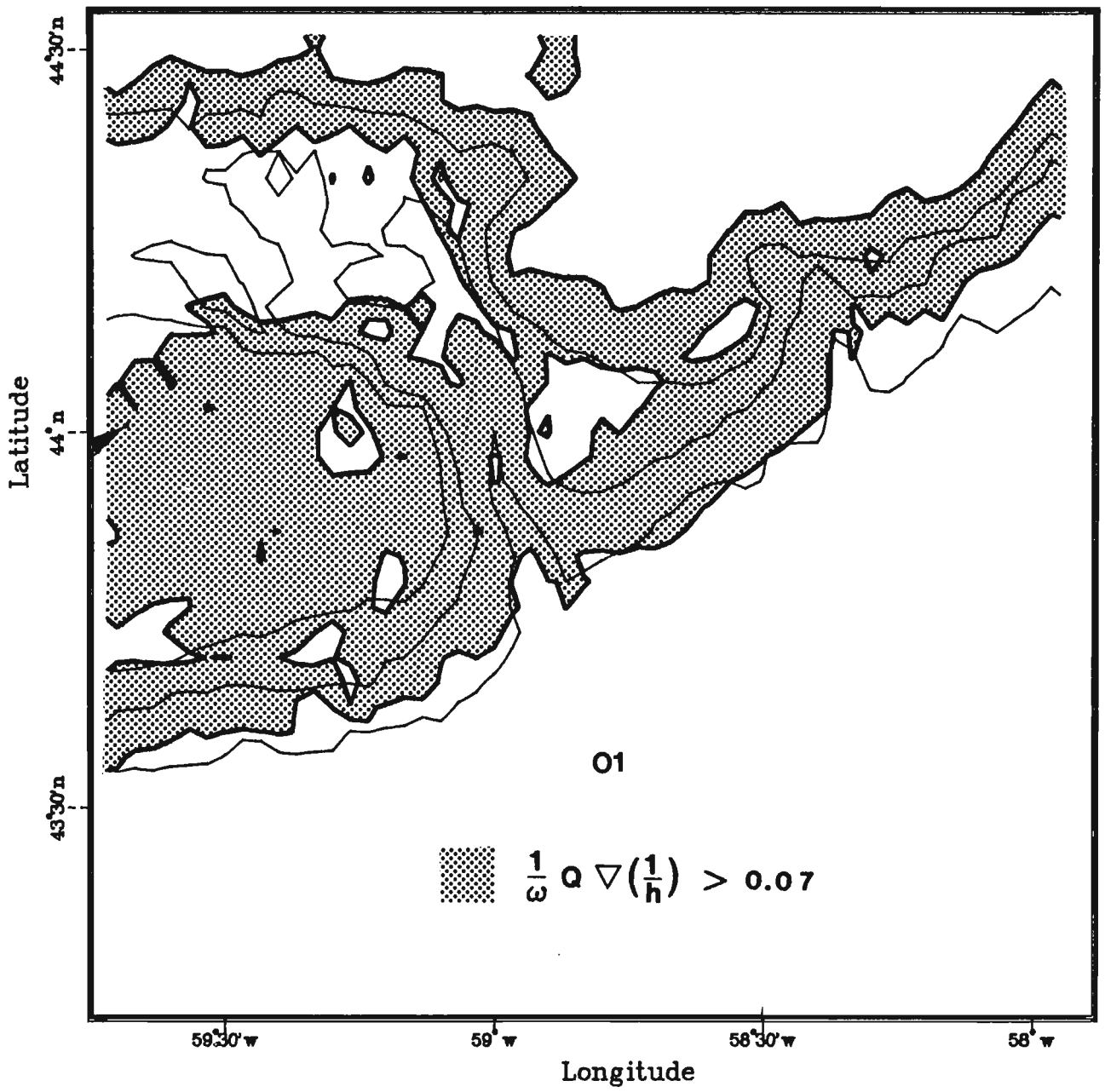
44°30'n
44°n
43°30'n
Latitude
59°30'w
59°w
58°30'w
58°w
Longitude
O1
$\frac{1}{\omega} Q \nabla\left(\frac{1}{h}\right) > 0.07$